

Supplementary Information

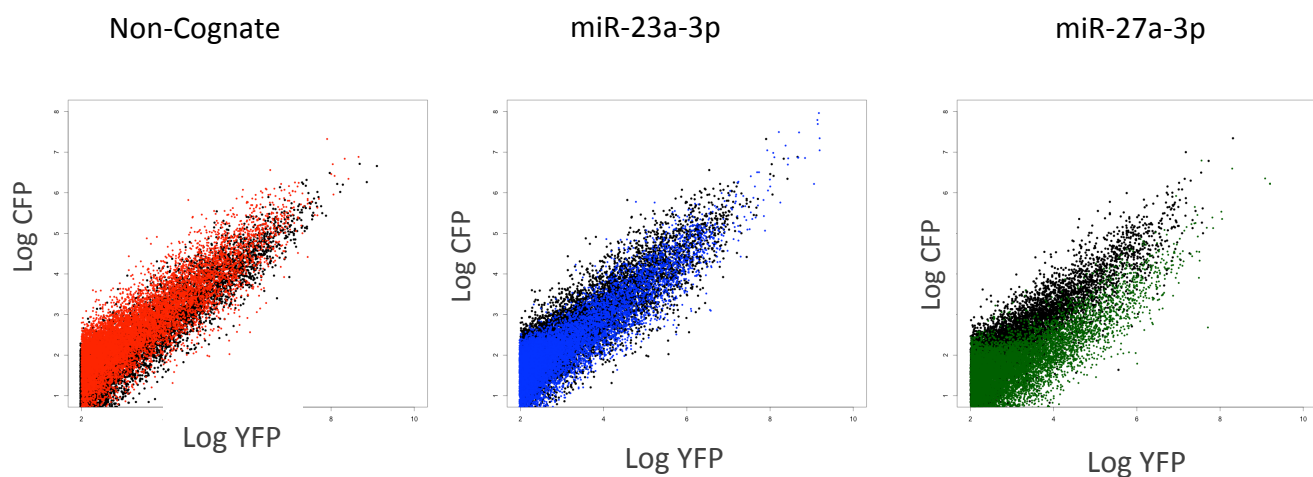
Dissecting miRNA gene repression on single cell level with an advanced fluorescent reporter system

Nicolas Lemus-Diaz, Kai O. Böker, Ignacio Rodriguez-Polo, Michael Mitter, Jasmin Preis, Maximilian Arlt, Jens Gruber

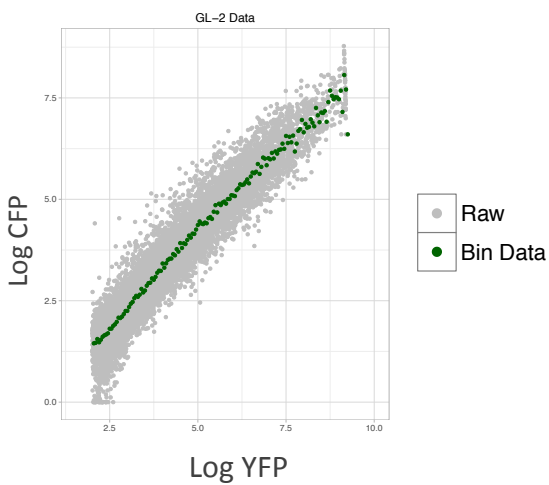
Junior Research Group Medical RNA Biology, German Primate Center, Kellnerweg 4, 37077 Göttingen, Germany

Figure. S1

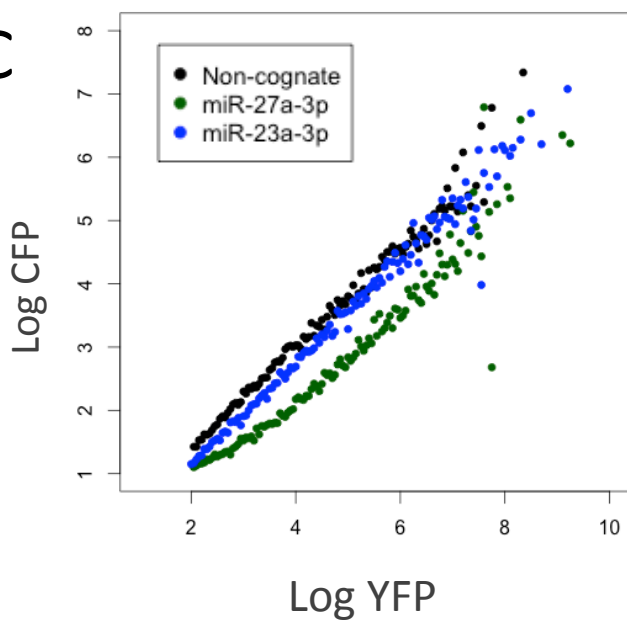
A



B



C



D

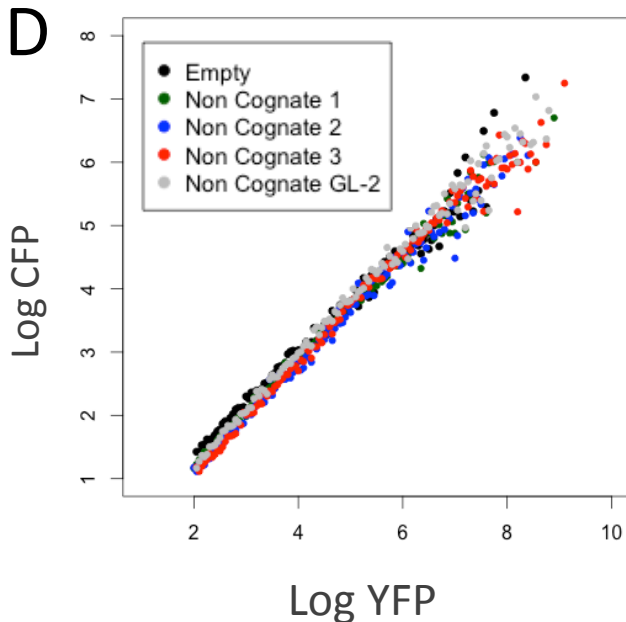


Figure S1: Dual Fluorescence Reporter System functionally characterized miRNA activity. Hek293 were transfected with 3 different sensor constructs (miR-23a-3p, miR-27a-3p and Non-cognate) and evaluated after 72 h. **(A)** FACS scatter plots of YFP positive cells from constructs containing the miR-23-a-3p (Blue), miR-27a-3p (green) and non-cognate (Red) targeted site and the empty vector is depicted in black. Single cell analysis transfer function generation: YFP intensities were binned (1 to 8 at 0.05 intervals) and the average of each bin was calculated, **(B)** scatter plot of the GL-2 targeted construct (grey) and the calculated transfer function (green) **(C)** Transfer Function for miR-27a-3p and miR-23a-3p and **(D)** Transfer function for Three different cognate controls.

Figure. S2

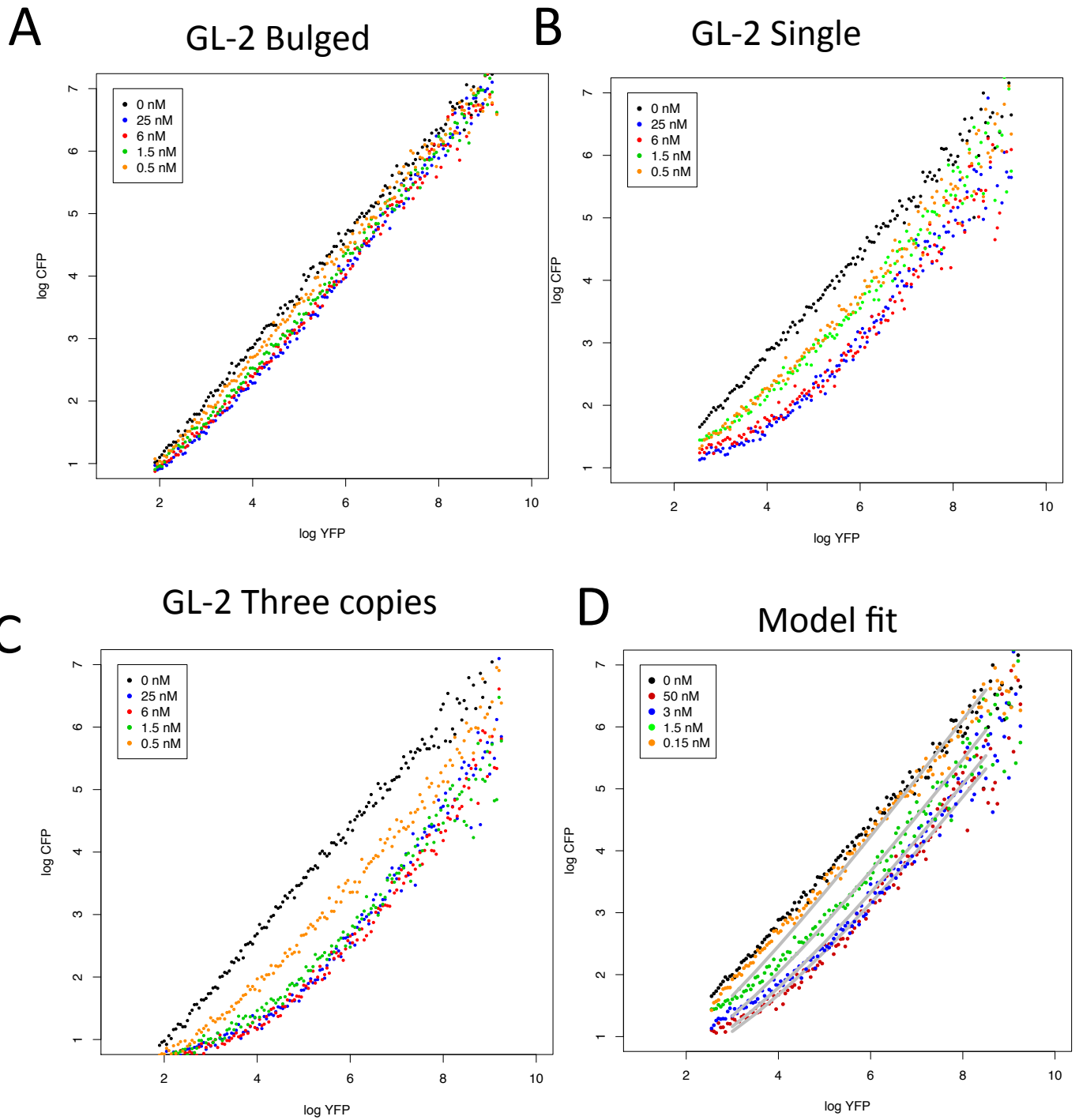


Figure S2: A molecular titration model for miRNA-mediated regulation describes different threshold behavior for siRNA activity. Simulation was experimentally tested using GL-2 binding site included in the dual fluorescence reporter assay. To test λ three different target sites were evaluated: (A) Bulged 19 exact base pair bulged with 3 unpaired bases (B) one 21 perfectly complementary bases and (C) Three 21 exact complementary binding sites separated by 4 unpaired bases. (D) Fit lines derived from the model using nonlinear (weighted) least squares.

Figure. S3

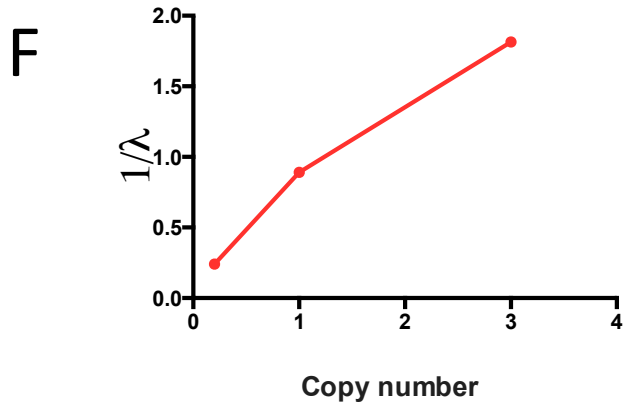
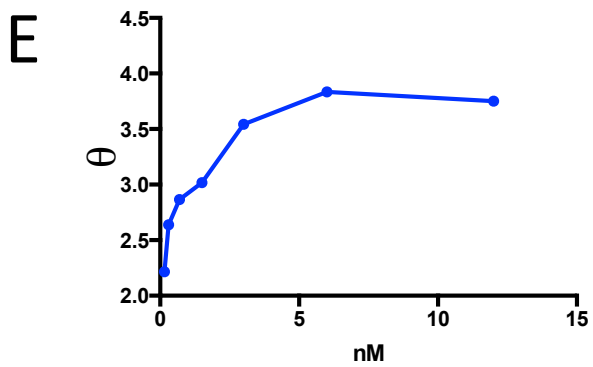
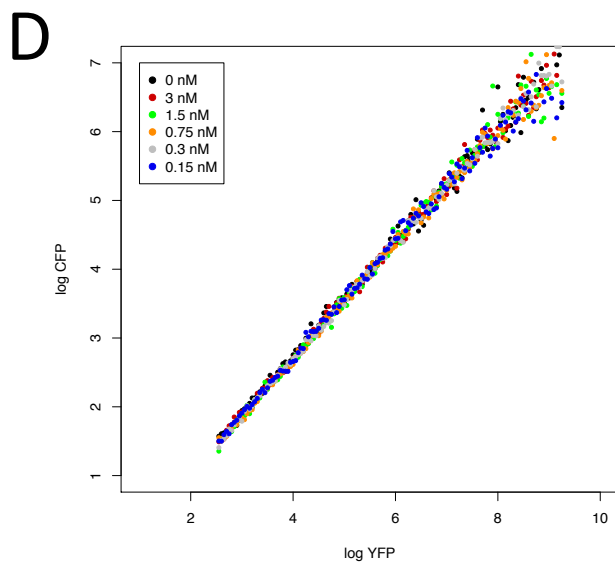
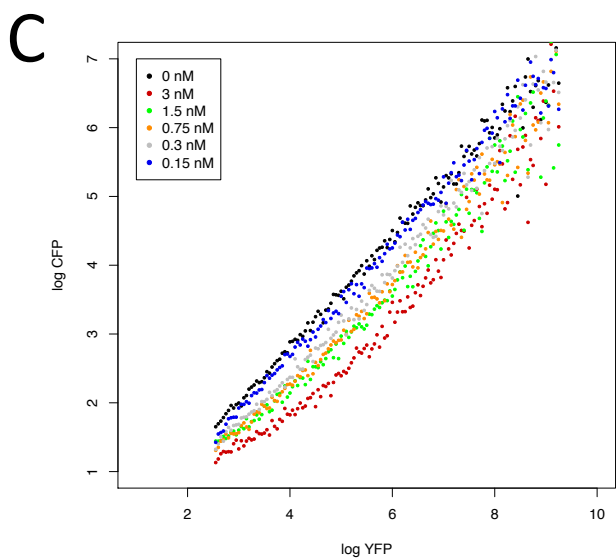
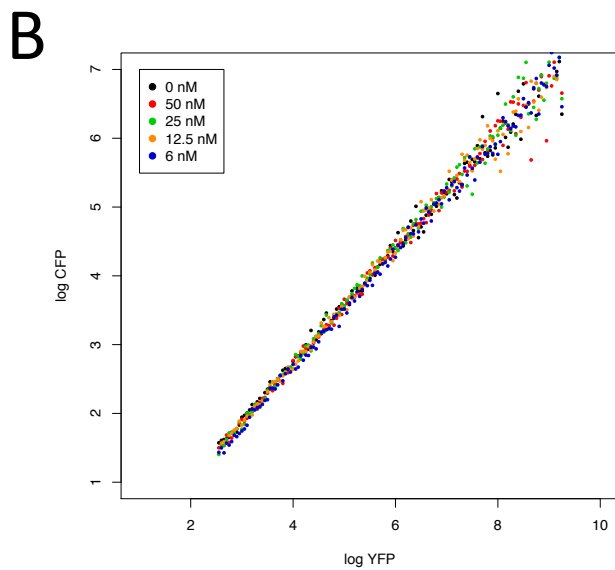
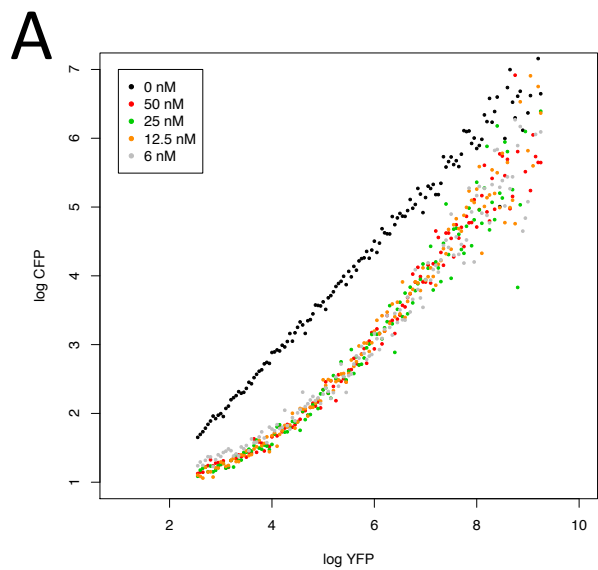


Figure S3: Experimental range definition of θ and λ . Dual Fluorescence Reporters for GL-2 and Non Cognate inserted sites were co-transfected in HEK293 with different concentration of GL-2 siRNA, after 72 h transfer functions were calculated: **(A)** GL-2 and **(B)** Non cognate targeted constructs co-transfected with 50 to 6 nM GL-2 siRNA. **(C)** GL-2 targeted and **(D)** Non-cognate targeted concentration construct co-transfected with 3 to 0.15 nM GL-2 siRNA.

Non-linear regression was performed to estimate θ and λ for all the GL-2 siRNA experiments: first constant λ (binding capability) was selected arbitrary to estimate θ from 50 to 12 nM siRNA, then it was averaged and plotted: **(E)** GL-2 siRNA Concentration vs. averaged estimated θ .

Estimated θ from 25 nM -GL-2 co-transfected was used to estimate λ for bulged, single and three copies constructs. **(E)** Copy number vs estimated $1/\lambda$, bulged was arbitrary set to 0.5.

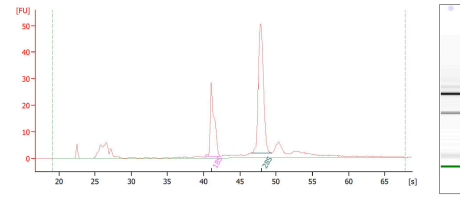
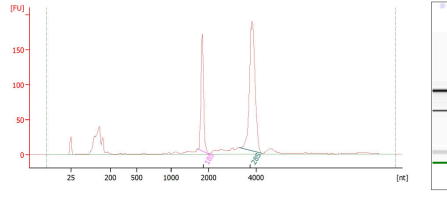
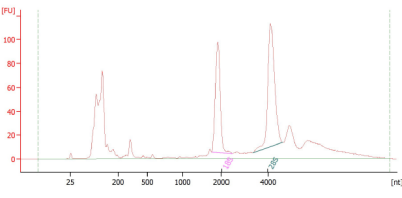
Figure. S4

Negative Control (BC1)
Hek 293-1

Negative Control (BC4)
Hek 293-2

Negative Control (BC7)
Hek 293-3

A

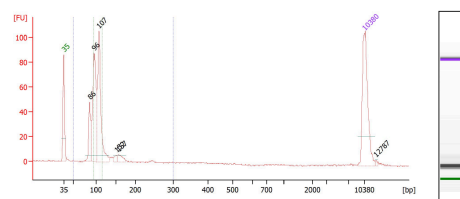
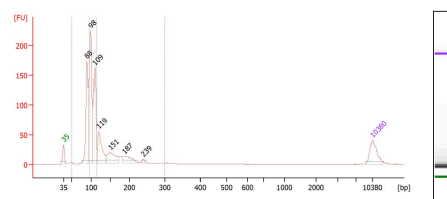
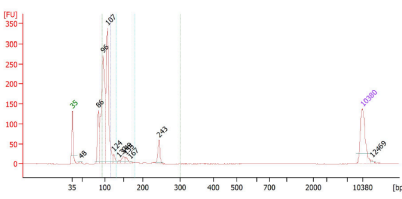


Overall Results for sample 1 : **A**
 RNA Area: 1,125.0
 RNA Concentration: 773 ng/ul
 rRNA Ratio [28s / 18s]: 1.3
 RNA Integrity Number (RIN): 9 (B.02.08)
 Result Flagging Color:
 Result Flagging Label: RIN:9

Overall Results for sample 1 : **28 ND control**
 RNA Area: 921.4
 RNA Concentration: 3,713 pg/ul
 rRNA Ratio [28s / 18s]: 1.9
 RNA Integrity Number (RIN): 9.8 (B.02.08)
 Result Flagging Color:
 Result Flagging Label: RIN:9.80

Overall Results for sample 3 : **Negative total**
 RNA Area: 226.5
 RNA Concentration: 185 ng/ul
 rRNA Ratio [28s / 18s]: 1.9
 RNA Integrity Number (RIN): 10 (B.02.08)
 Result Flagging Color:
 Result Flagging Label: RIN:10

B



C

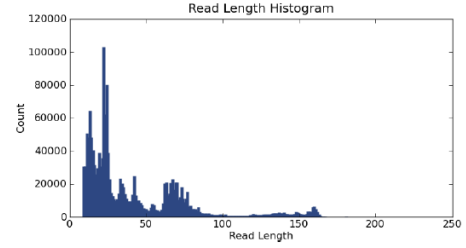
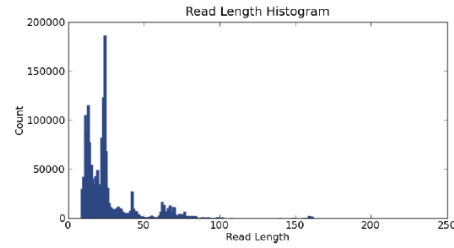
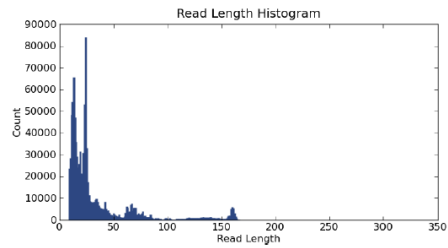
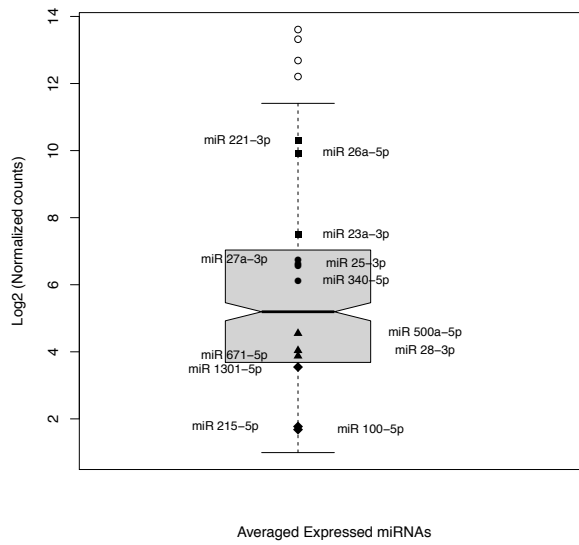


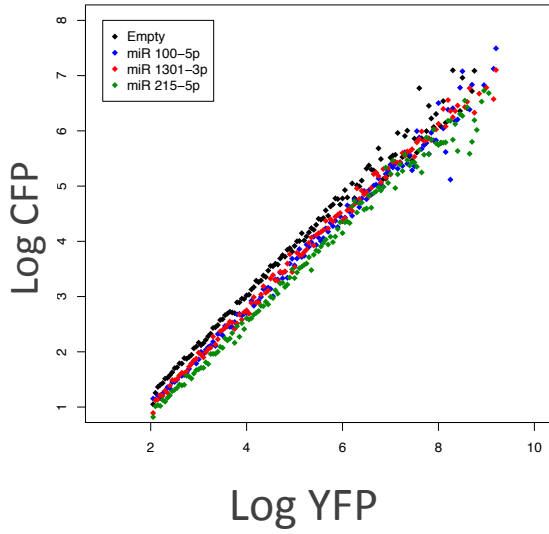
Figure S4: RNA quality control and library size distribution. Three independent total RNA isolations were performed and RNA integrity tested by BioAnalyzer System **(A)**. If RNA integrity number (RIN) was higher than 9 **(B)** Ion Torrent small RNA library preparation were performed and quantified and **(C)**. Diluted library (18 pM) was sequenced via IonTorrent System.

Figure. S5

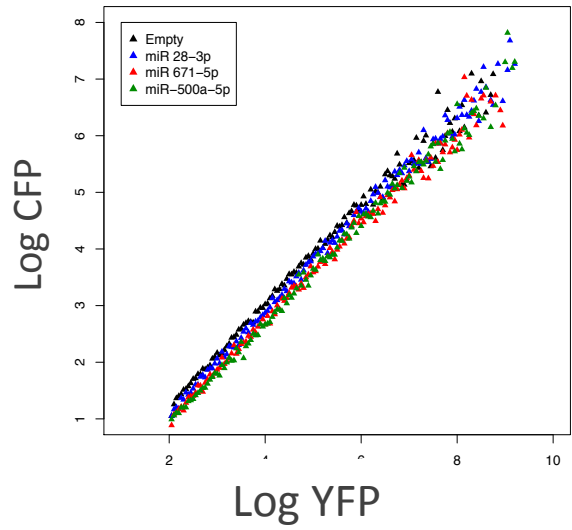
A



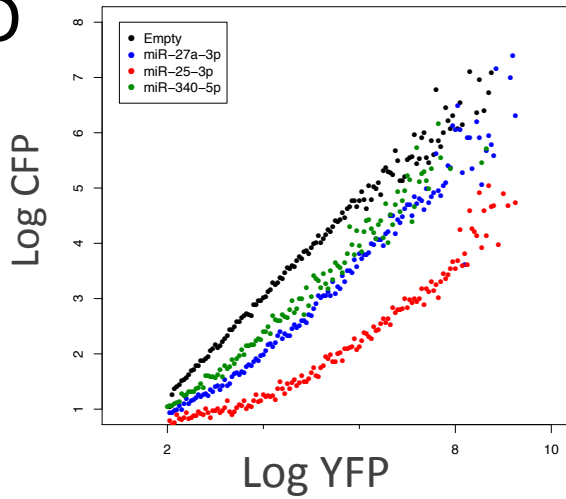
B



C



D



E

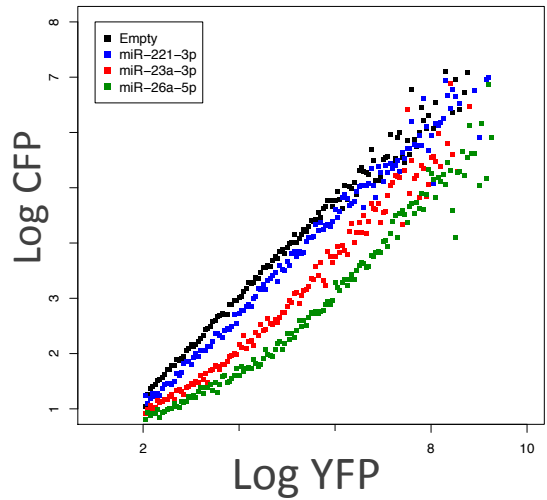
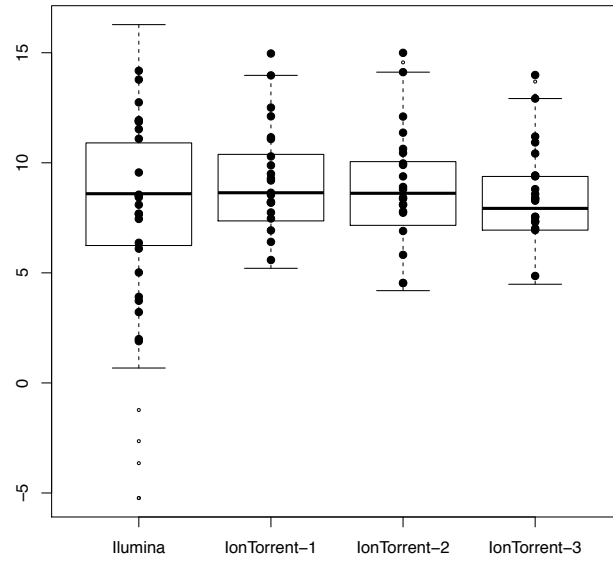


Figure S5: Dual Fluorescence Reporter System UTA is suitable for single cell measurements of endogenous miRNAs. Three miRNAs libraries from 3 independent Hek293 cultures were sequenced by IonTorrent platform and **(A)** twelve different miRNAs were selected based on their expression levels (Mean Normalized Counts) and quartile position, then 12 different reporters for were generated and functionally tested using FACS. UTA Transfer function for candidates located: **(B)** below the first quartile, **(C)** between the median and the first quartile, **(C)** above median and the third quartile; **(D)** above the third quartile.

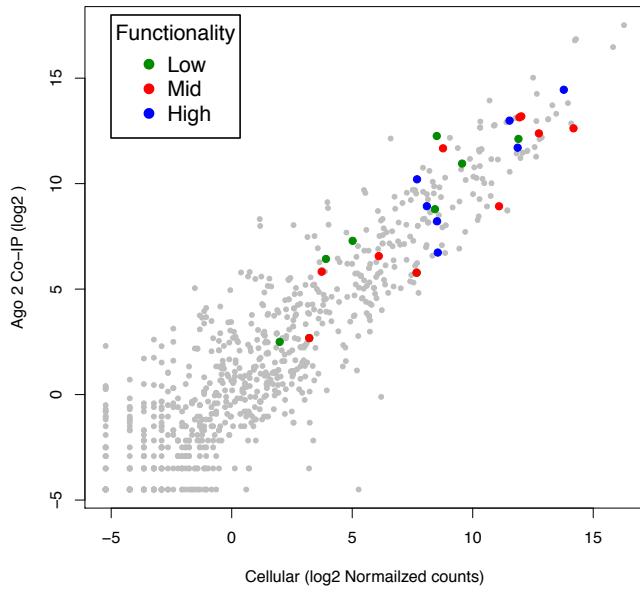
Figure. S6

A



B

Abcam ab57113



C

diagenode 2A8

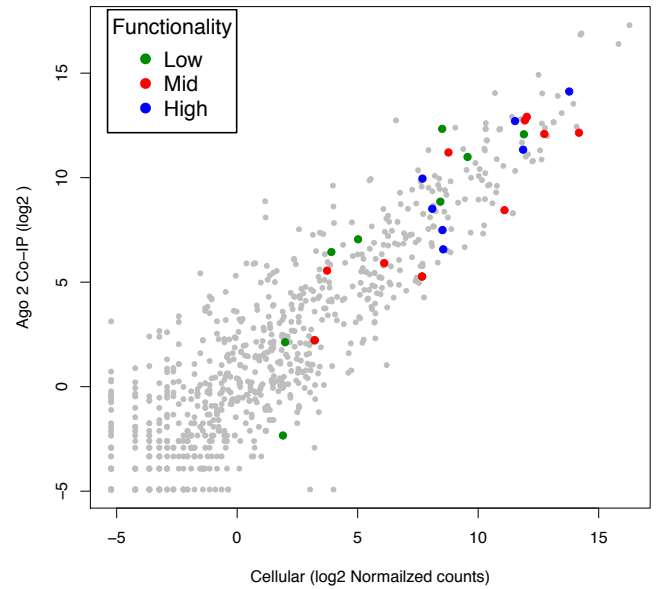
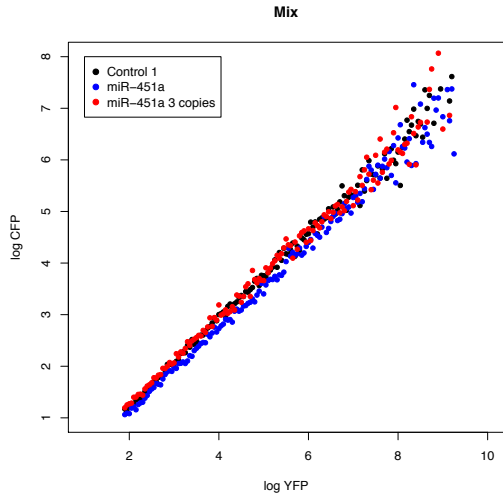


Figure S6: AGO2 miRNA association does not explain functional groups from dual fluorescence reporters. Read count tables from HEK293 total cellular content and AGO2 IP RNA were retrieved from (<http://www.ncbi.nlm.nih.gov/geo/query/acc.cgi?acc=GSE58127>). Tested miRNAs are similar distributed between NGS platforms: Illumina platform: **(A)** miRNA Data from HEK293 cells (GSE58127) Libraries were normalized by RPKM together with the Ion Torrent produced libraries in this study; miRNA distribution was plotted using Box plot and tested miRNAs are depicted as bold points.

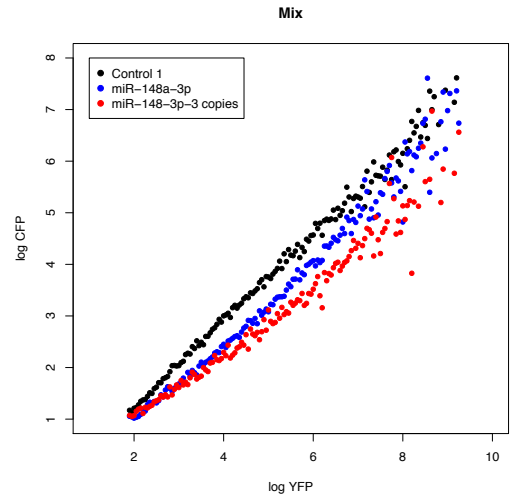
AGO2 Co-IP data from two independent antibodies were compared with total cellular miRNA content Read counts plotted total cellular content vs. (B) Antibody Abcam57113 and (C) Diogenode 2A8; functional groups are depicted on green (low functional), red (Mid functional), blue (High Functional).

Figure. S7

A



B



C

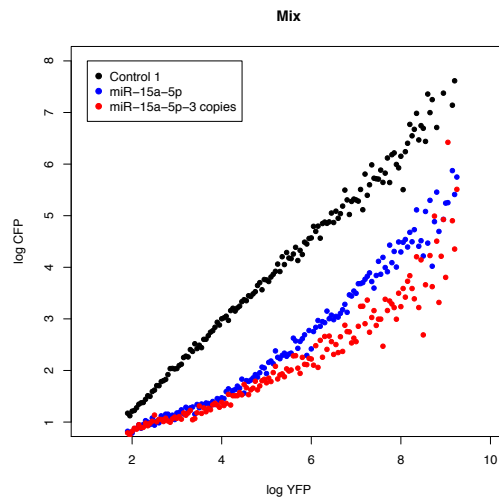
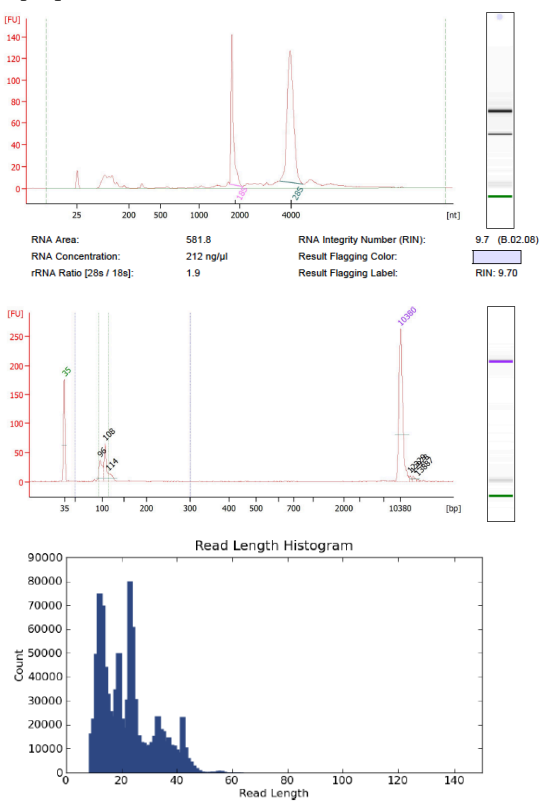
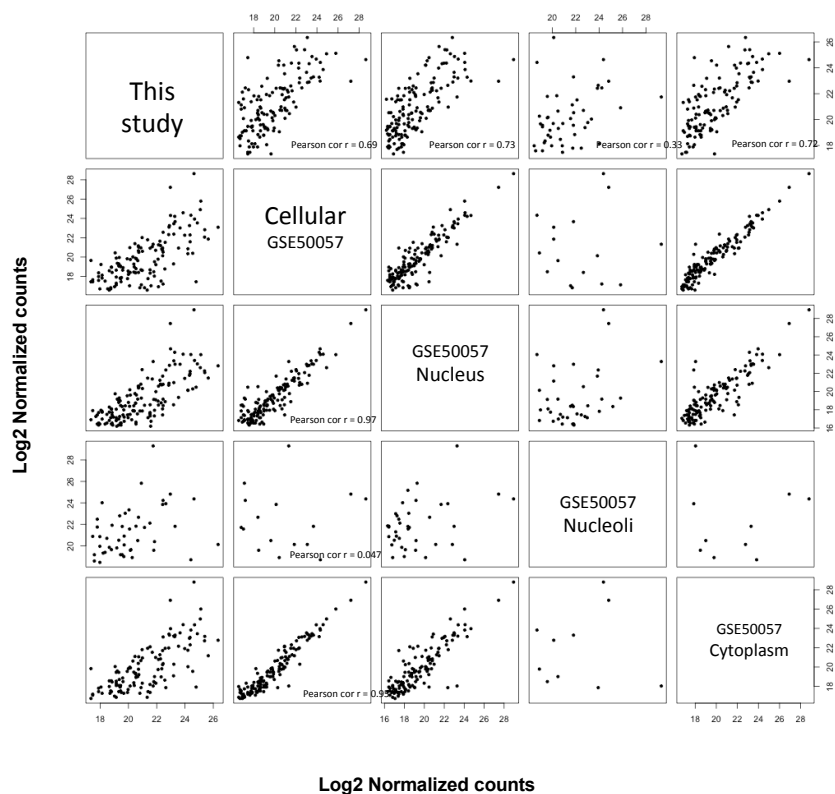


Figure S7 Threshold modulation of endogenous miRNAs: Three miRNAs were selected (one for each functional group) and one and three copies of perfect complementarity were inserted in UTA reporter. HEK293 cells were transfected and evaluated after 72 h. **(A)** Low functional miRNA, **(B)** mid Functional miRNA and **(C)** High Functional RNA.

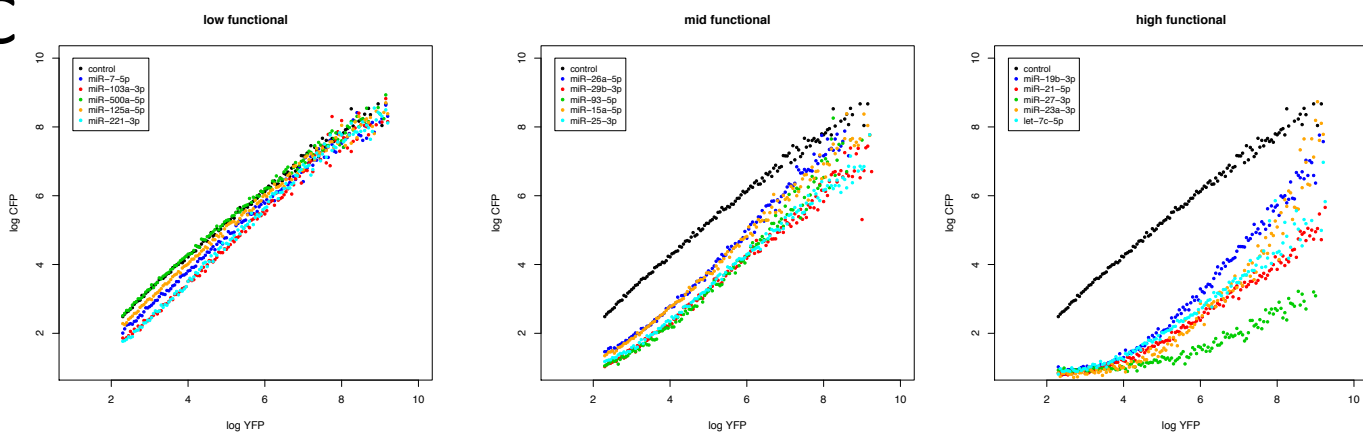
A Figure. S8



B



C



D

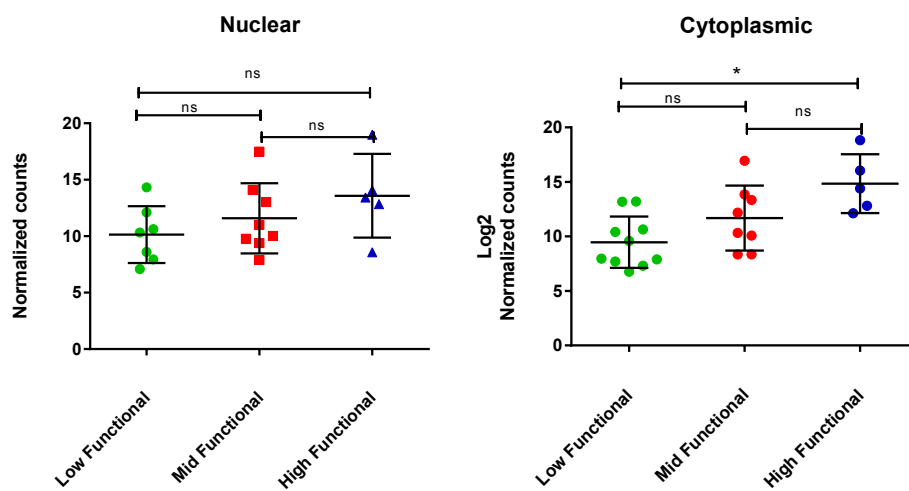


Figure S8. Functional characterization of miRNAs from single cell reporter assays in HeLa cells. **(A)** Bionalyzer graphs for total RNA quality, prepared library and read distribution of sequenced library from HeLa cells. GSE50057 raw data and produced library were aligned to miRNA and snoRNA database, **(B)** Scatter plot from normalized reads with Pearson correlation between the used libraries.

All tested HEK293 miRNAs reporters were transfected in HeLa cells and UTA transfer function generated: **(C)** miRNA functional outputs were classified as before low functional (left), mid functional (center) and high functional (right). **(D)** Read count distribution for the three ordinal qualitative groups for Nuclear (left) and Cytoplasmic (right) libraries.

Supplementary Table 1: DNA oligonucleotides used in this study.

miRNA	Oligos (5'-3' XhoI or NotI overhangs)
hsa-miR-100-5p	ggccagcttctttacagtgccttg
	tcgacaaggcagcactgtaaagaagct
hsa-miR-1301-3p	ggcctgcagctgcctgggagtgacttc
	tcgagaagtactcccaggcagctgca
hsa-miR-215-5p	ggccatgacatgaattgacagac
	tcgagtctgtcaattcataggcat
hsa-miR-28-3p	ggcccactagattgtgagctcctgga
	tcgatccaggagctcacaatctagtg
hsa-miR-29a-3p	ggcctagcacatctgaaatcggtta
	tcgataaccgatttcagatggtgcta
hsa-miR-24-3p	ggcctggctcagttcagcaggaacag
	tcgactgttctgctgaactgagcca
hsa-miR-451a	ggccaaaccgttaccattactgagtt
	tcgaaactcagtaatggtaacggttt
hsa-miR 7-5p	ggcctggaagactagtgattttgtgt
	tcgaacaacaaaatcactagtctcca
hsa-miR-15a-5p	ggcctagcagcacataatggtttgtg
	tcgacacaaaccattatgtgctgcta
hsa-miR-19b-3p	ggcctgtgcaaatccatgcaaaactga
	tcgatcagtttgcatggattgcaca
hsa-miR-26a-5p	ggcctcaagtaatccaggataggct
	tcgaagcctatcctggattactgaa
hsa-miR-29b-3p	ggcctagcaccatttgaaatcagtggt
	tcgaaacactgattcaaatggtgcta
hsa-miR-93-5p	ggcccaaagtgtgttcgtgcaggtag
	tcgactacctgcacgaacagcactttg
hsa-miR-103a-3p	ggccagcagcattgtacagggctatga
	tcgatcatagccctgtacaatgtgct
hsa-miR-148a-3p	ggcctcagtgactacagaactttgt
	tcgaacaaagttctgtagtgcactga
hsa-miR-181a-5p	ggccaacattcaacgctgtcggtgagt
	tcgaactaccgacagcgttgaatgtt
hsa-miR-221-3p	ggccagctacattgtctgctgggttc
	tcgagaaaccagcagacaatgtagct
hsa-let-7c-5p	ggcctgaggtagtaggtgtatggtt
	tcgaaaccatacaacctactacctca
hsa-miR-18a-5p	ggcctaagggtcatctagtgcagatag
	tcgactatctgcactagatgcacctta
hsa-miR-19b-3p	ggcctgtgcaaatccatgcaaaactga
	tcgatcagtttgcatggattgcaca
hsa-miR-25-3p	ggcccattgcactgtctcgggtctga
	tcgatcagaccgagacaagtgcaatg

hsa-miR-125a-5p	ggcctccctgagaccctttaacctgtga
	tcgatcacagggttaaagggctcagggga
hsa-miR-500a-5p	ggcctaataccttgctacctgggtgaga
	tcgatctcaccaggtagcaaggatta
hsa-miR-340-5p	ggccttataaagcaatgagactgatt
	tcgaaatcagtctcattgctttataa
hsa-miR-671-5p	ggccaggaagccctggaggggctggag
	tcgactccagccccctccagggtctct
hsa-miR-3607-5p	ggccgcatgtgatgaagcaaatcagt
	tcgaaactgattgcttcatcacatgc
hsa-miR-3607-3p	ggccactgtaaacgctttctgatg
	tcgacatcagaaagcgtttacagt
hsa-miR-21-5p	ggcctagcttatcagactgatgtga
	tcgatcaacatcagtctgataagcta
hsa-miR-27a 3-p	ggccttcacagtggttaagtccgc
	tcgagcggaacttagccactgtgaa
hsa-miR-23a 3-p	ggccatcacattgccagggattcc
	tcgaggaaatccctggcaatgtgat
hsa-miR-27a 3-p bulged	ggccttcacaggtctaagtccgc
	tcgagcggaacttagacctgtgaa
GL-2	ggcccacgtacgcggaataacttcgaaa
	tcgatttcgaagtattccgcgtacgtg
GL-2 bulged	ggcccacgtacgcggttacttcgaaa
	tcgatttcgaagtagaccgcgtacgtg

Supplementary Table 2: Summarized data of miRNA expression, functional classifications and results of transfer function regression

miRNAs	Functional Group*	Lambda ^{1,3}	Theta ¹	Normalized Read Counts ²
hsa-miR-7-5p	MF	1,5	3,4	192,3
hsa-miR-103a-3p	MF	1,3	3,2	1949,3
hsa-miR-148a-3p	MF	2,1	3,1	193,6
hsa-miR-181a-5p	MF	3,0	3,6	188,4
hsa-miR-221-3p	MF	1,0	3,0	1249,9
hsa-miR-340-5p	MF	2,3	3,2	107,6
hsa-miR-27a-3p	MF	2,7	4,0	70,0
hsa-miR-100-5p	LF	4,0	3,1	3,2
hsa-miR-1301-3p	LF	3,7	2,9	11,7
hsa-miR-215-5p	LF	2,6	2,9	3,4
hsa-miR-28-3p	LF	3,9	2,6	16,4
hsa-miR-29a-3p	LF	2,2	2,7	94,2
hsa-miR-24-3p	LF	2,3	3,2	261,1
hsa-miR-29b-3p	LF	1,9	3,0	352,0
hsa-miR-451a	LF	8,0	3,9	0,0
hsa-miR-125a-5p	LF	2,3	3,2	239,8
hsa-miR-500a-5p	LF	4,8	3,4	23,4
hsa-miR-671-5p	LF	5,7	4,0	14,7
hsa-miR-3607-5p	LF	4,0	3,5	456,4
hsa-miR-3607-3p	LF	3,6	3,1	439,8
hsa-miR-23a-3p	LF	1,6	2,3	180,7
hsa-miR-15a-5p	HF	1,7	5,1	424,3
hsa-miR-19b-3p	HF	1,7	7,0	12501,7
hsa-miR-26a-5p	HF	1,2	3,9	969,5
hsa-miR-93-5p	HF	1,6	6,0	1365,8
hsa-let-7c-5p	HF	1,3	5,5	131,9
hsa-miR-18a-5p	HF	1,1	6,0	6586,8
hsa-miR-25-3p	HF	1,4	6,0	98,2
hsa-miR-21-5p	HF	2,6	5,6	585,5

*Low Functional= LF, Mid Functional=MF, High Functional=HF.

1.Lambda and Theta values were calculated using non-linear least squares.

2.Counts were Normalized using the DEseq Package on R.

3.Lambda ($\lambda \sim K_{off}$ or $\lambda \sim 1/K_{on}$)

Supplementary Table 3: Summarized data of miRNA expression and functional classification for HeLa Cells. Data retrieved from GEO GSE50057*

miRNA	Cellular	Nu	Cyto	No	Ratio	Function
hsa_let_7c_5p	1977,11	382,08	4471,07	NA	11,70	HF
hsa_miR_100_5p	7445,34	4400,72	9448,87	NA	2,15	LF
hsa_miR_103a_3p	19423,79	20570,80	9289,89	NA	0,45	LF
hsa_miR_125a_5p	1371,51	1275,87	765,05	29529,546	0,60	LF
hsa_miR_1301_3p	133,59	NA	NA	NA	#VALUE!	LF
hsa_miR_148a_3p	507,64	388,90	248,39	NA	0,64	LF
hsa_miR_15a_5p	400,77	238,80	327,88	NA	1,37	MF
hsa_miR_181a_5p	2333,35	1582,89	1361,19	1139,508	0,86	LF
hsa_miR_18a_5p	21009,04	17377,72	14883,70	NA	0,86	MF
hsa_miR_19b_3p	8905,91	7361,82	7163,65	NA	0,97	HF
hsa_miR_21_5p	417215,12	519530,32	466690,51	3678,984	0,90	HF
hsa_miR_221_3p	1059,80	245,62	1609,59	NA	6,55	LF
hsa_miR_23a_3p	58057,62	17241,26	67354,22	NA	3,91	HF
hsa_miR_24_3p	155844,50	183356,42	126402,18	NA	0,69	MF
hsa_miR_25_3p	1416,04	880,14	1082,99	NA	1,23	MF
hsa_miR_26a_5p	1994,92	668,64	4659,85	423,246	6,97	MF
hsa_miR_27a_3p	16039,54	11052,97	21679,73	1139,508	1,96	HF
hsa_miR_28_3p	NA	NA	158,97	NA	#VALUE!	LF
hsa_miR_29a_3p	605,60	1037,07	327,88	NA	0,32	LF
hsa_miR_29b_3p	5423,70	2067,31	1281,71	NA	0,62	MF
hsa_miR_500a_5p	106,87	NA	208,65	NA	#VALUE!	LF
hsa_miR_671_5p	418,58	NA	238,46	21650,659	#VALUE!	LF
hsa_miR_7_5p	NA	136,46	109,29	NA	0,80	LF
hsa_miR_93_5p	13323,24	8303,37	10333,14	NA	1,24	MF

*Bai, B., Yegnasubramanian, S., Wheelan, S. J. & Laiho, M. RNA-Seq of the nucleolus reveals abundant SNORD44-derived small RNAs. *PLoS one* 9, e107519, doi:10.1371/journal.pone.0107519 (2014).

Supplementary Information

Model Simulation online tool:

<https://medicalrbiology.shinyapps.io/pUTApp/>

$$r = 1/2(r_0 - \lambda - \theta + \sqrt{(r_0 - \lambda - \theta)^2 + 4\lambda r_0})$$

where:

$$r_0 = \frac{K_R}{y_R} \quad \lambda = \frac{y_{R^*} + K_{off}}{K_{on}} \quad \theta = \frac{y_{R^*}}{y_R} [miRNA]_T$$

Steady state solutions for r (log CFP) as a function of r₀ (log YFP)
Theta and Lambda can be introduced.

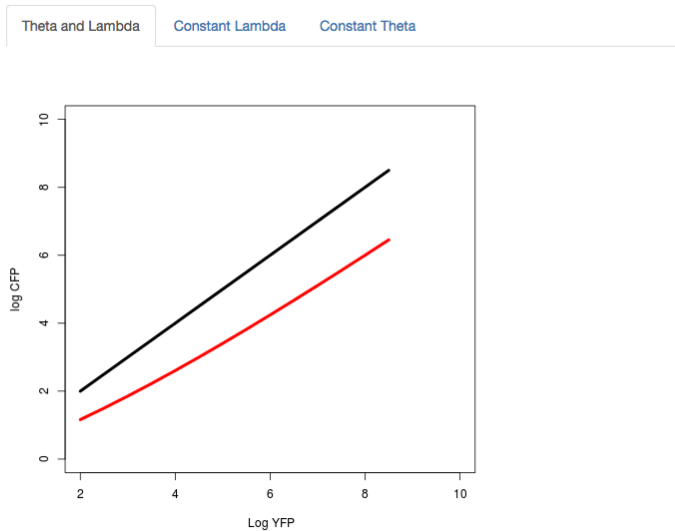
Simulation miRNA function

Give Theta

Theta is proportional to miRNA concentration

Give Lambda

Lambda is Inverse proportional to Kon



Several Theta values are computed (simulating miRNA concentration increments).

Simulation miRNA function

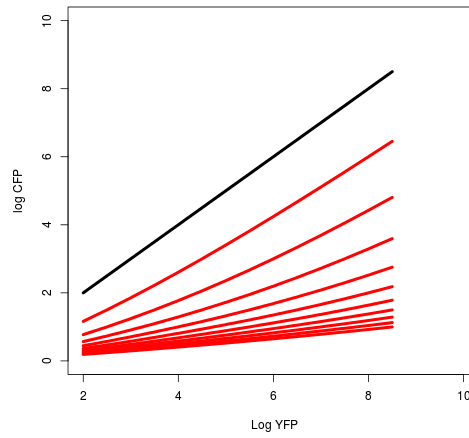
Give Lambda

Lambda is constant and inversely proportional to Kon

Theta and Lambda

Constant Lambda

Constant Theta



Several lambda values are computed (simulating changes on miRNA binding capability).

Simulation miRNA function

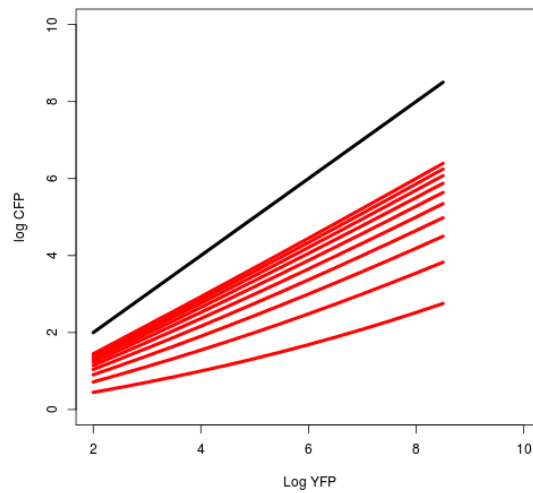
Give Theta

Theta is constant and proportional to [miRNA]

Theta and Lambda

Constant Lambda

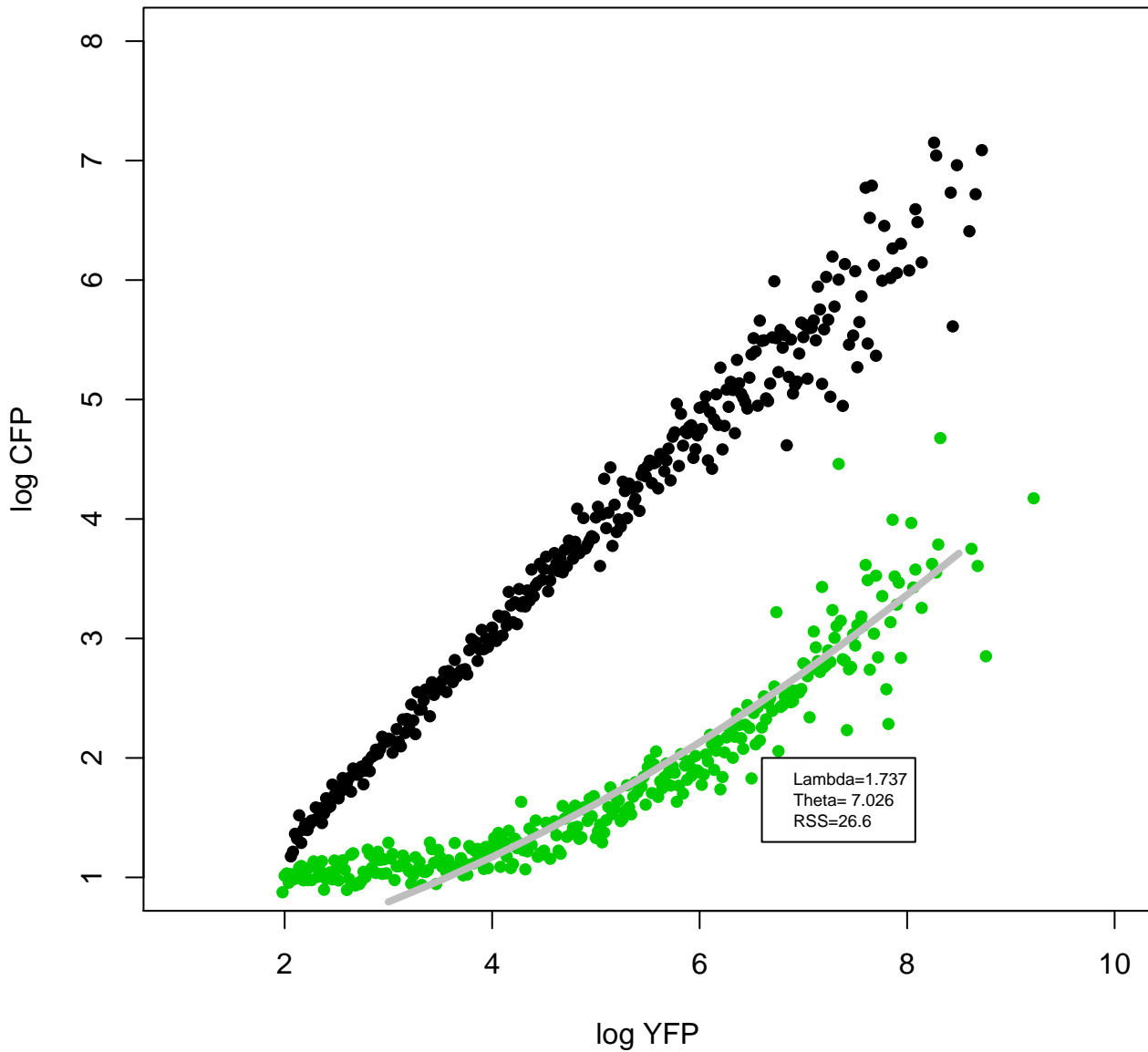
Constant Theta



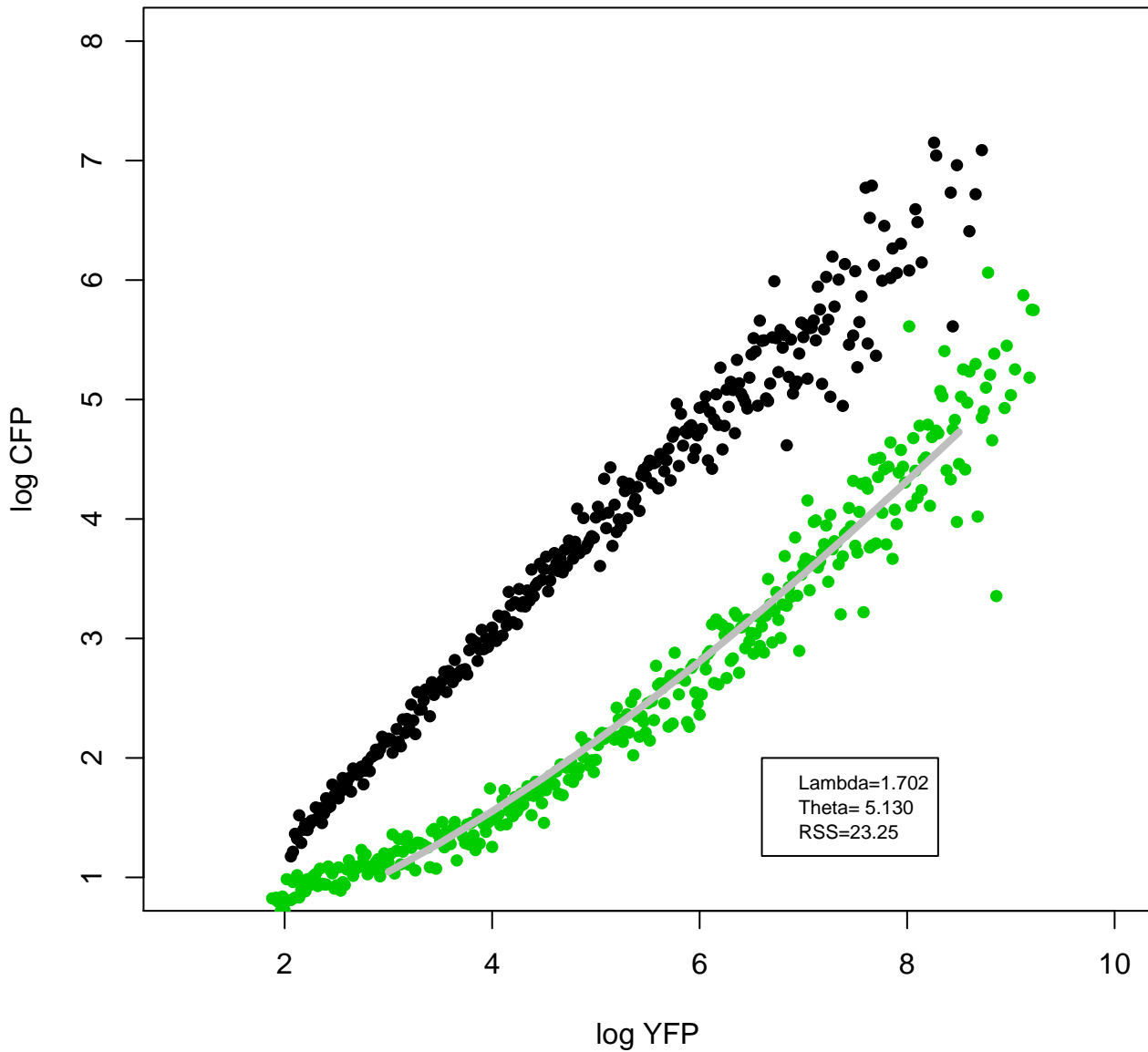
Supplementary extended data

All tested miRNA transfer function were calculated reduction bin size from 0.05 to 0.02. Non-linear regression was performed using least squares. Transfer function for miRNA are depicted in Green and Non-cognate control in black. Lambda ,Values and RSS are included.

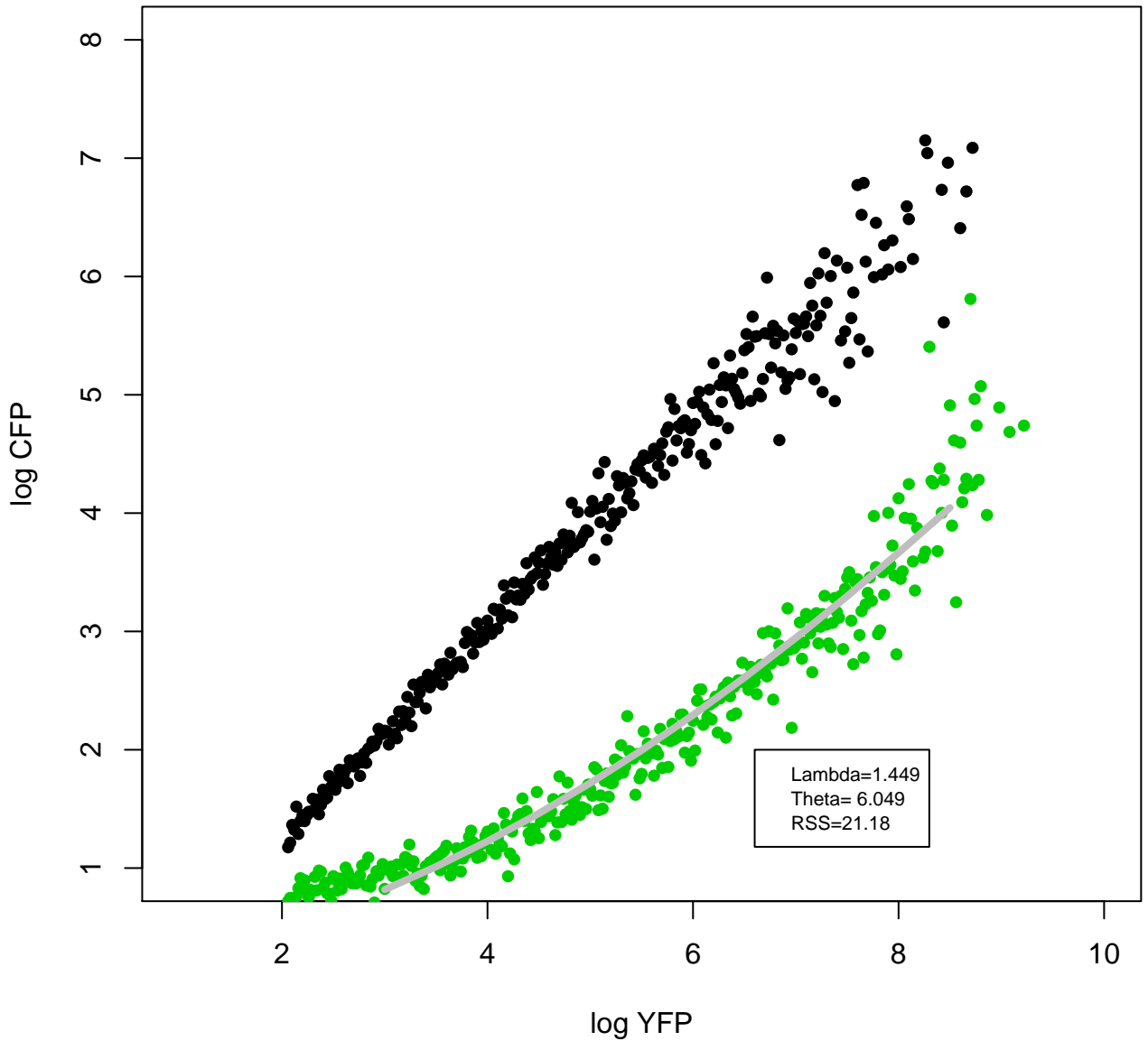
hsa-miR-19b-3p



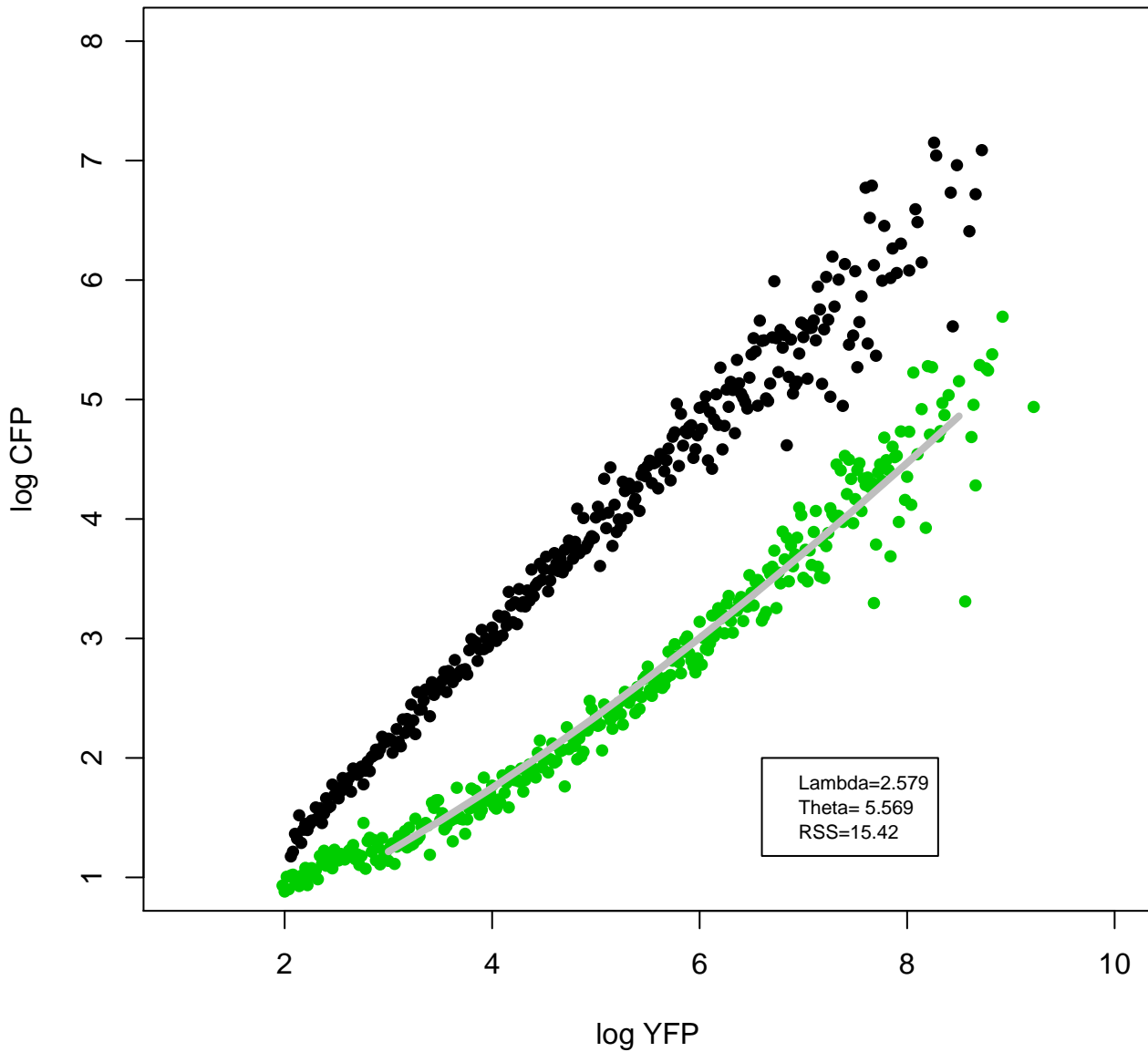
hsa-miR-15a-5p



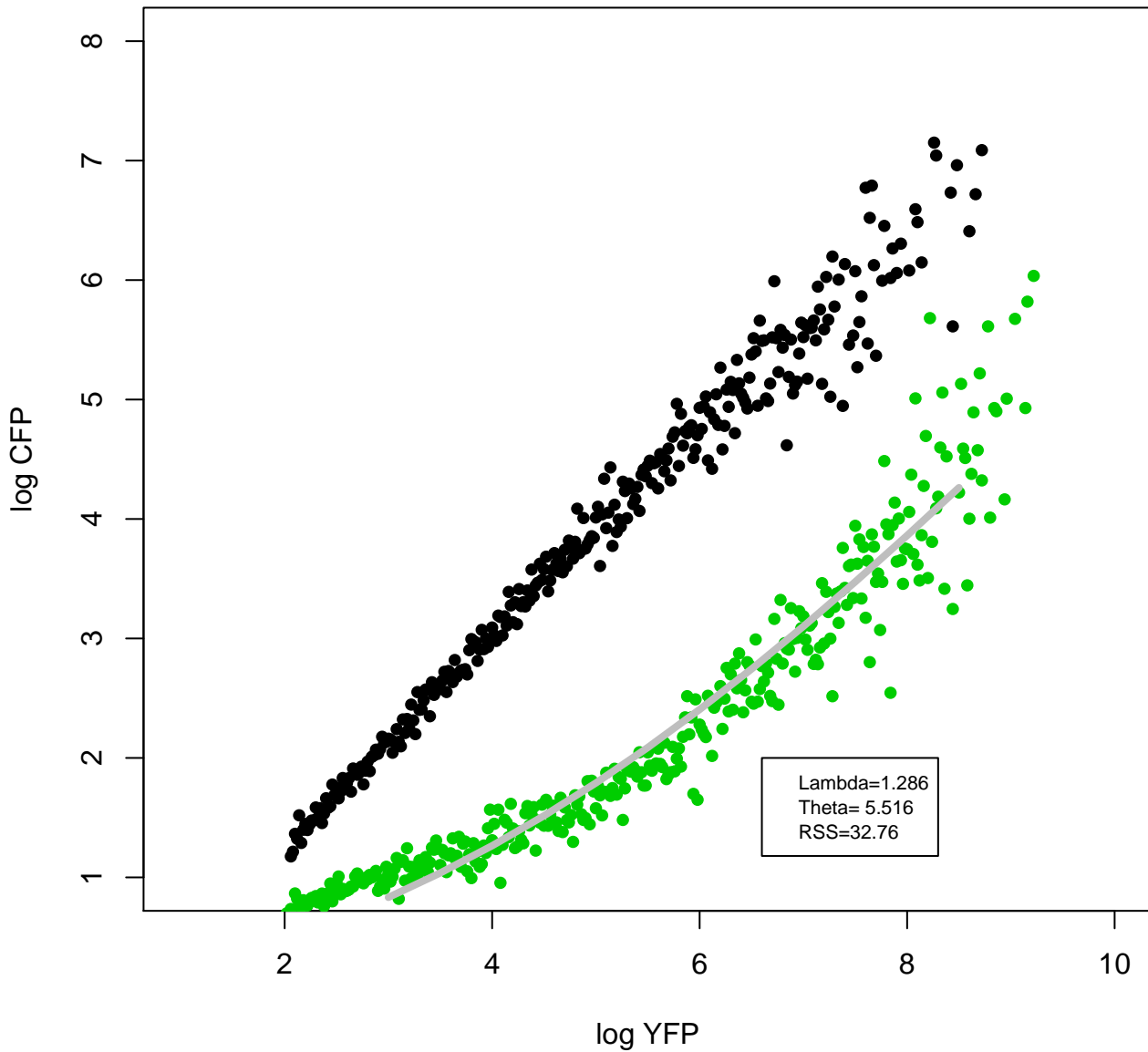
hsa-miR-25-3p



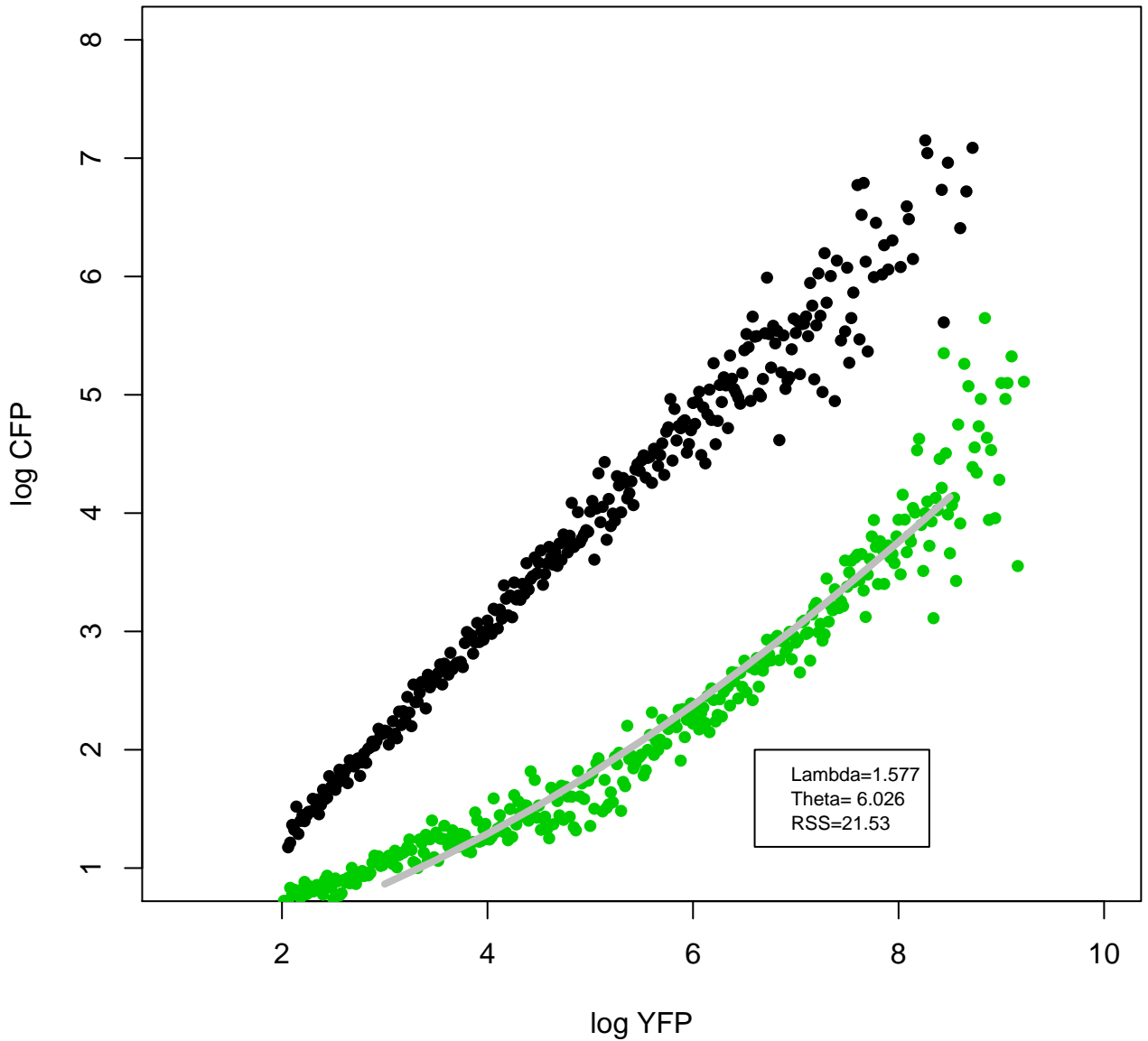
hsa-miR-21a-5p



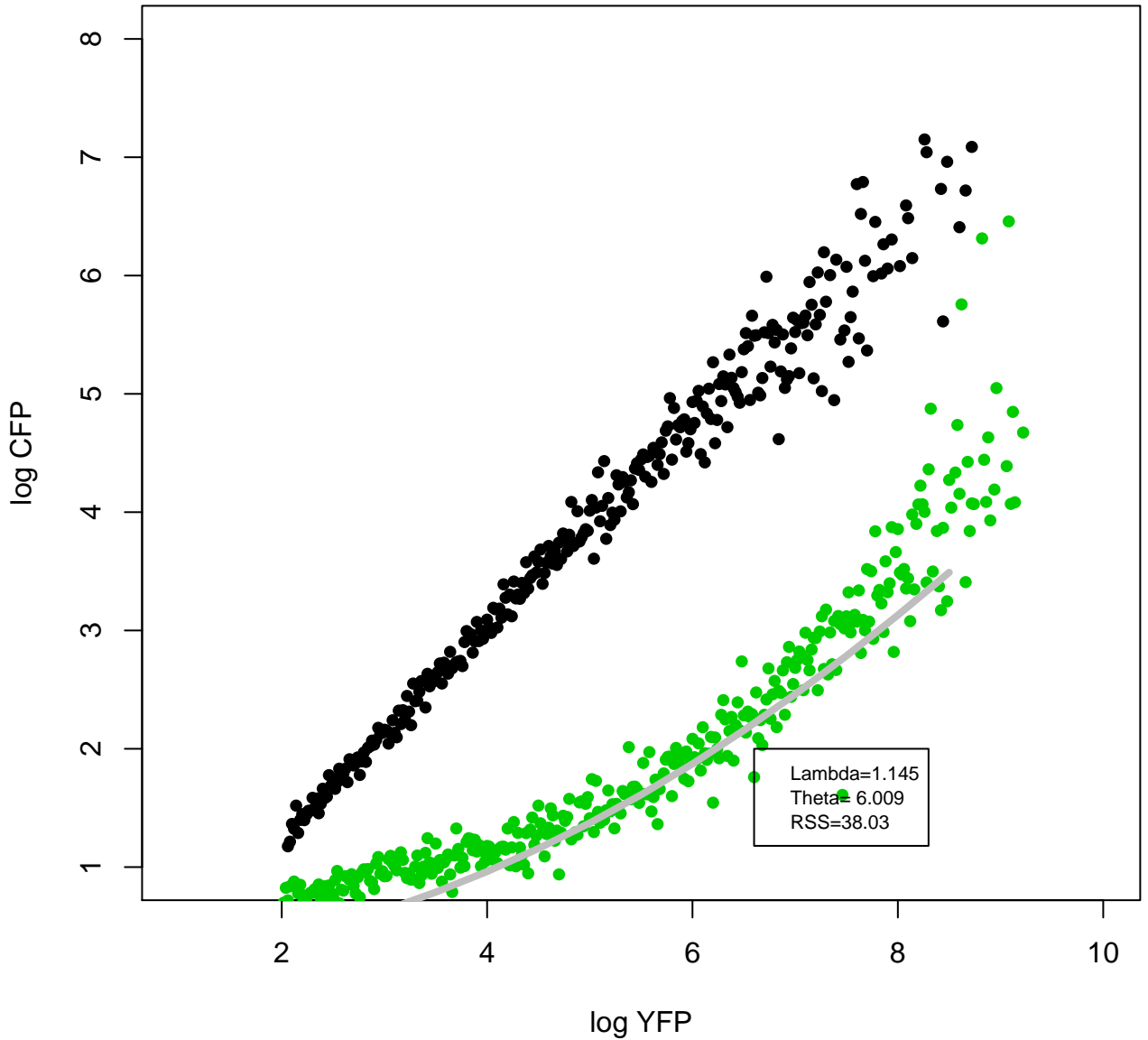
let-7c-5p



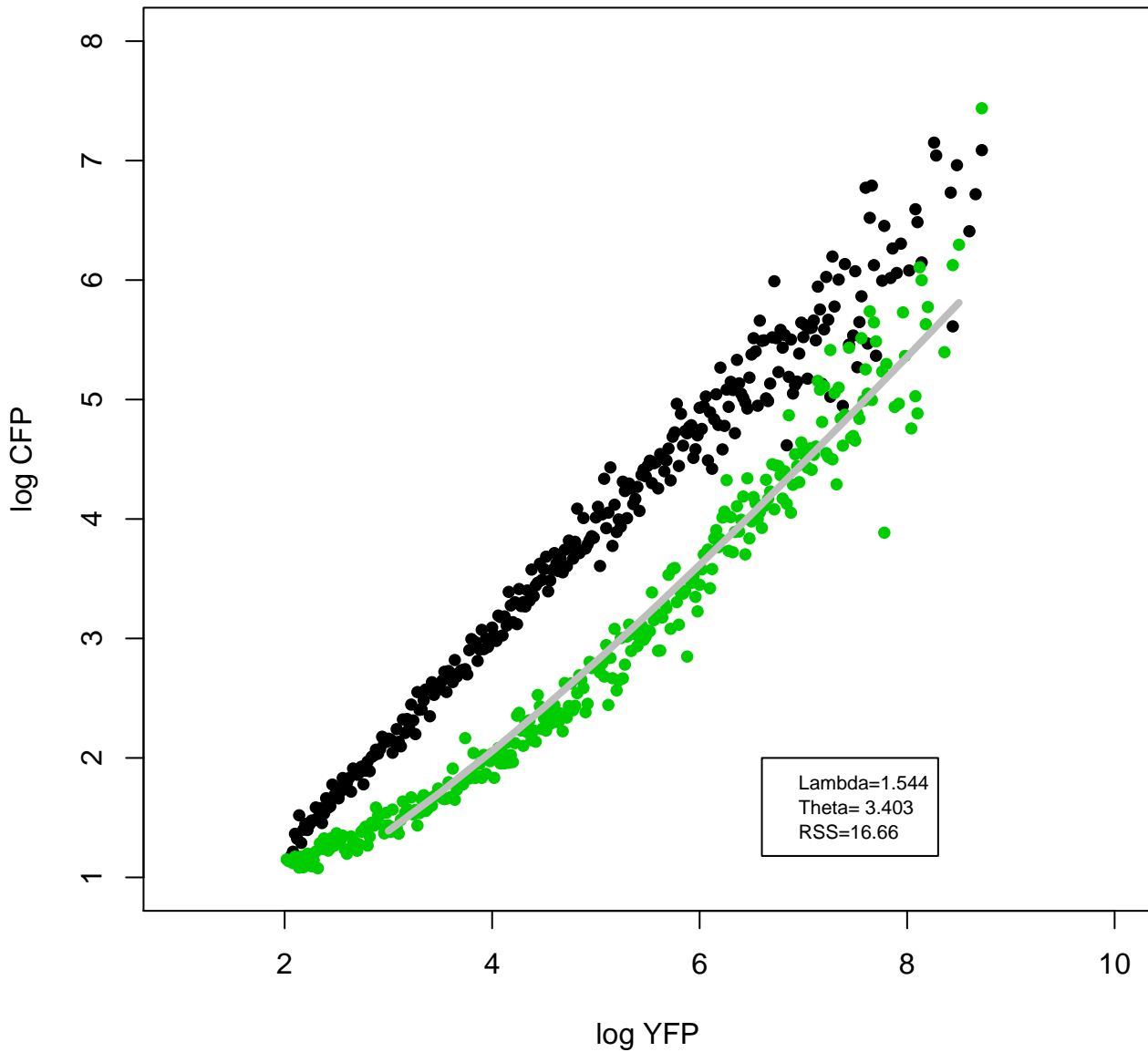
hsa-miR-93-5p



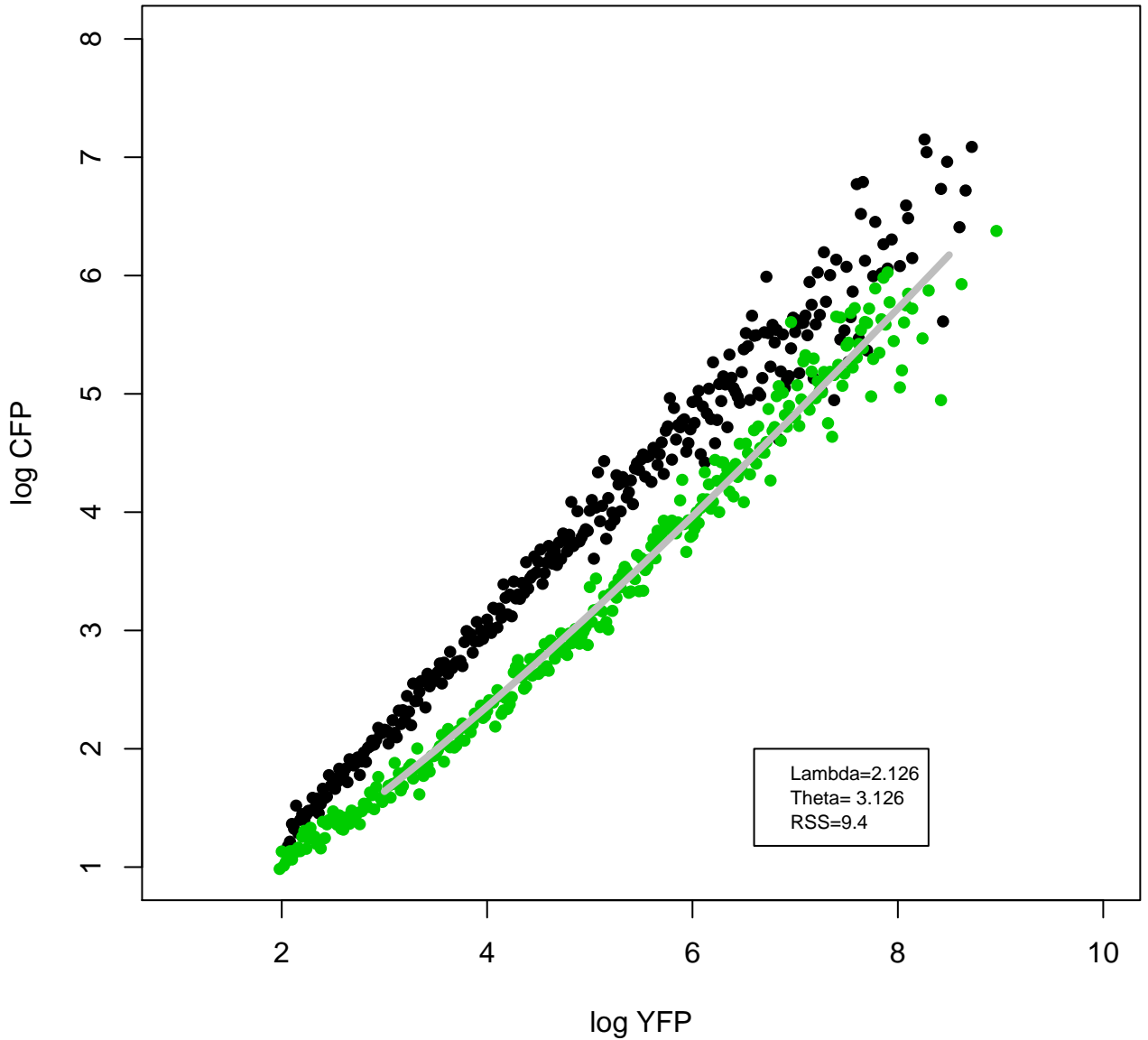
hsa-miR-18-5p



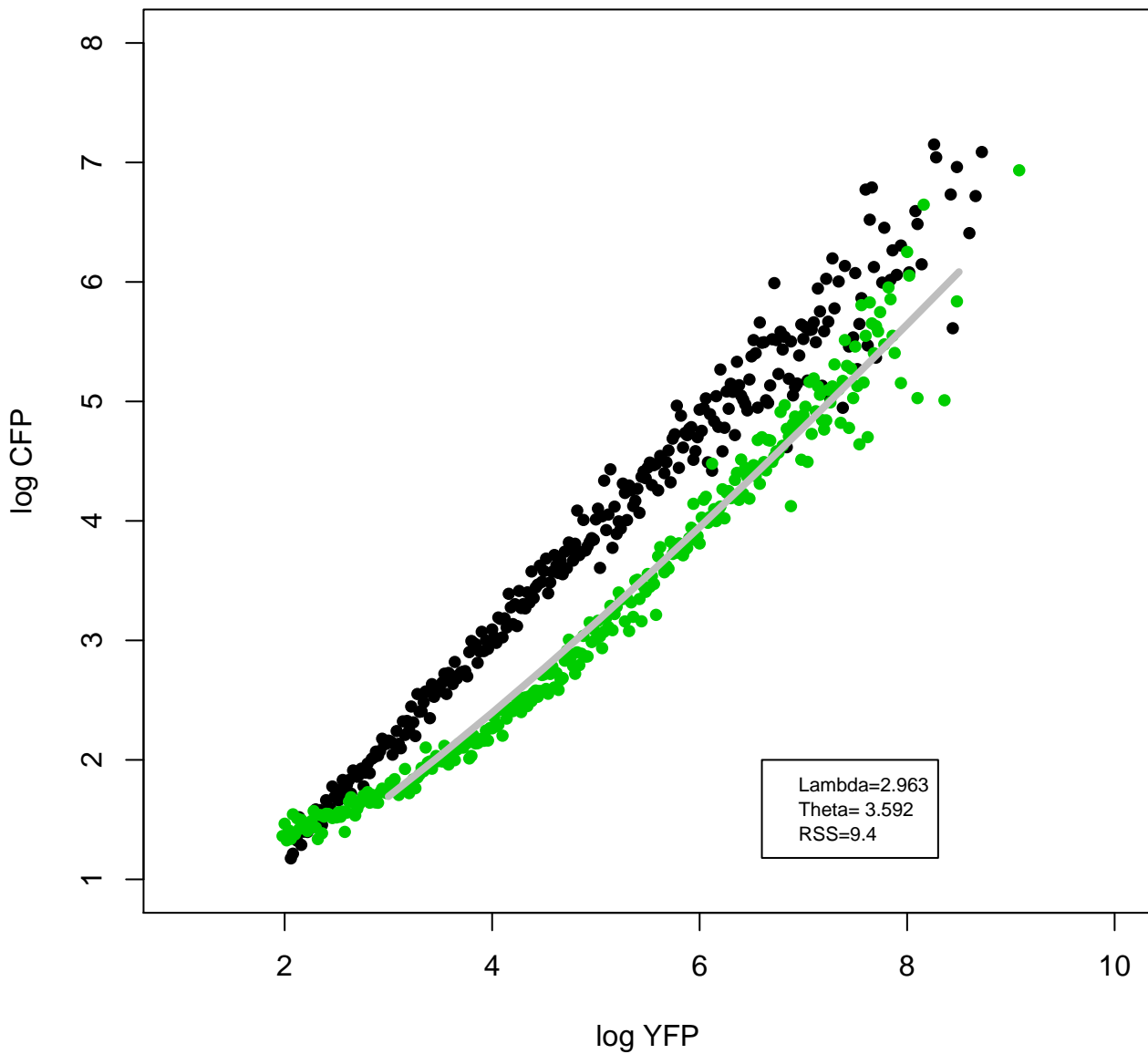
miR-7-5p



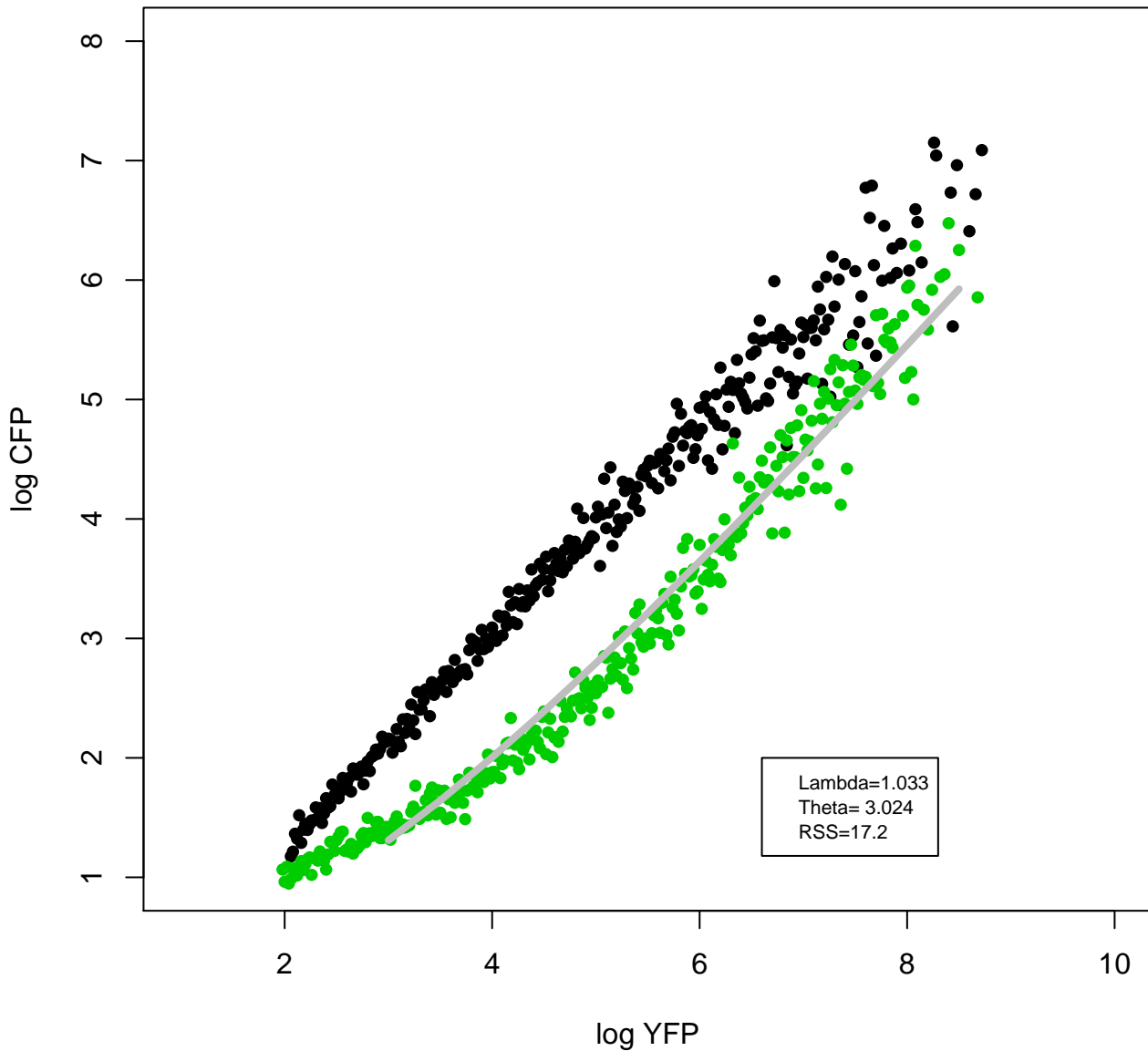
hsa-miR-148a-3p



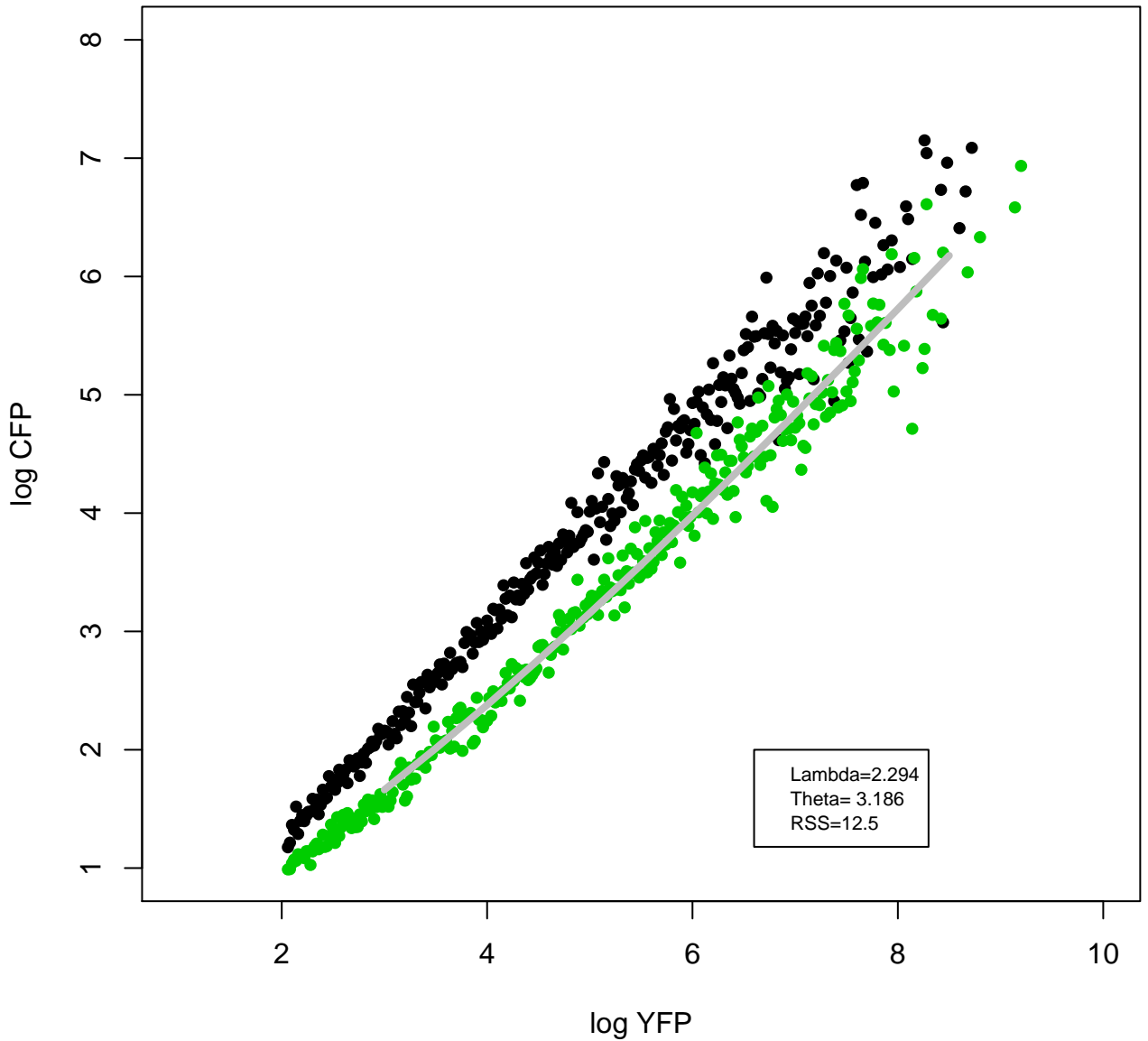
hsa-miR-181a-5p



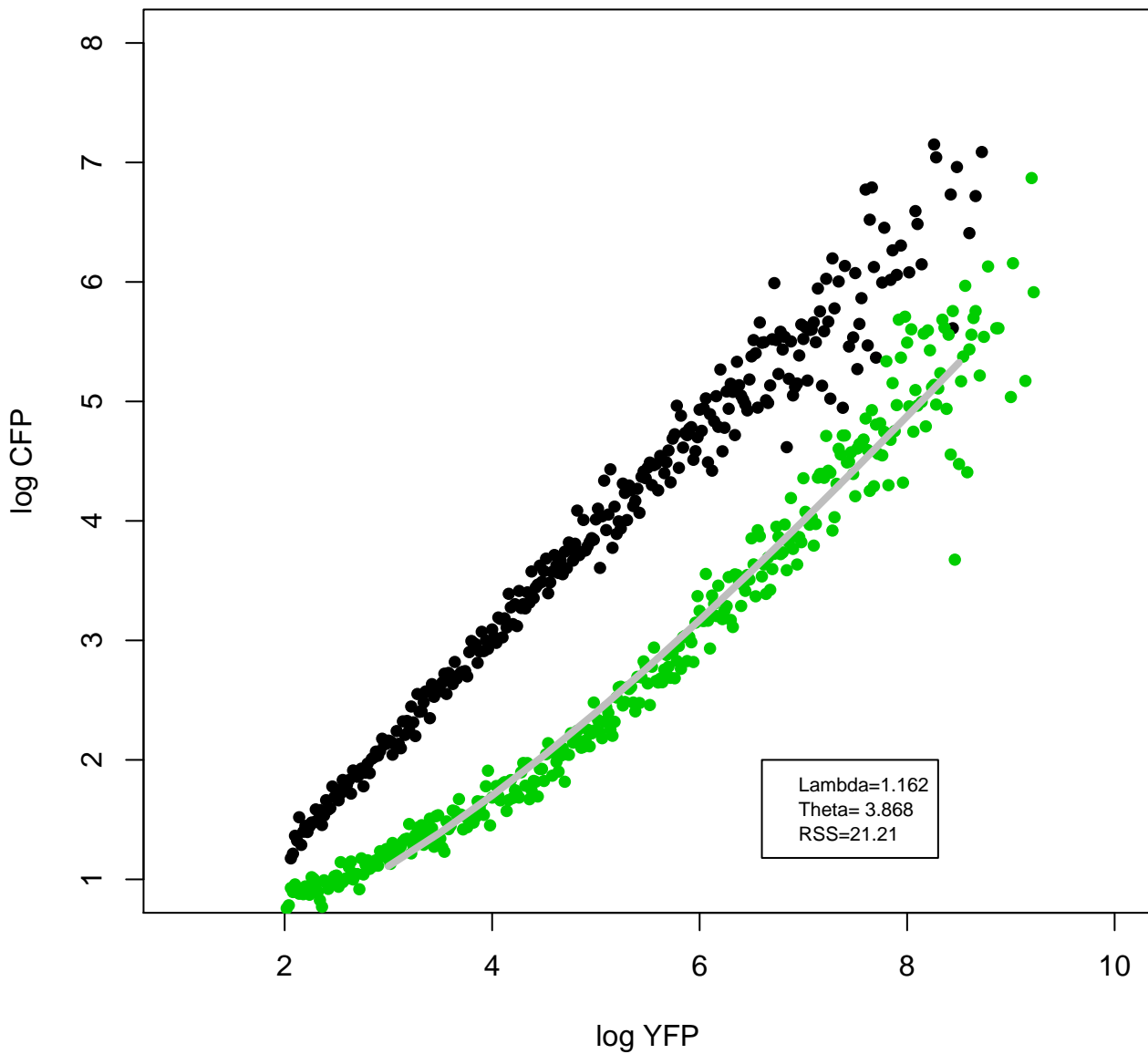
hsa-miR-221-3p



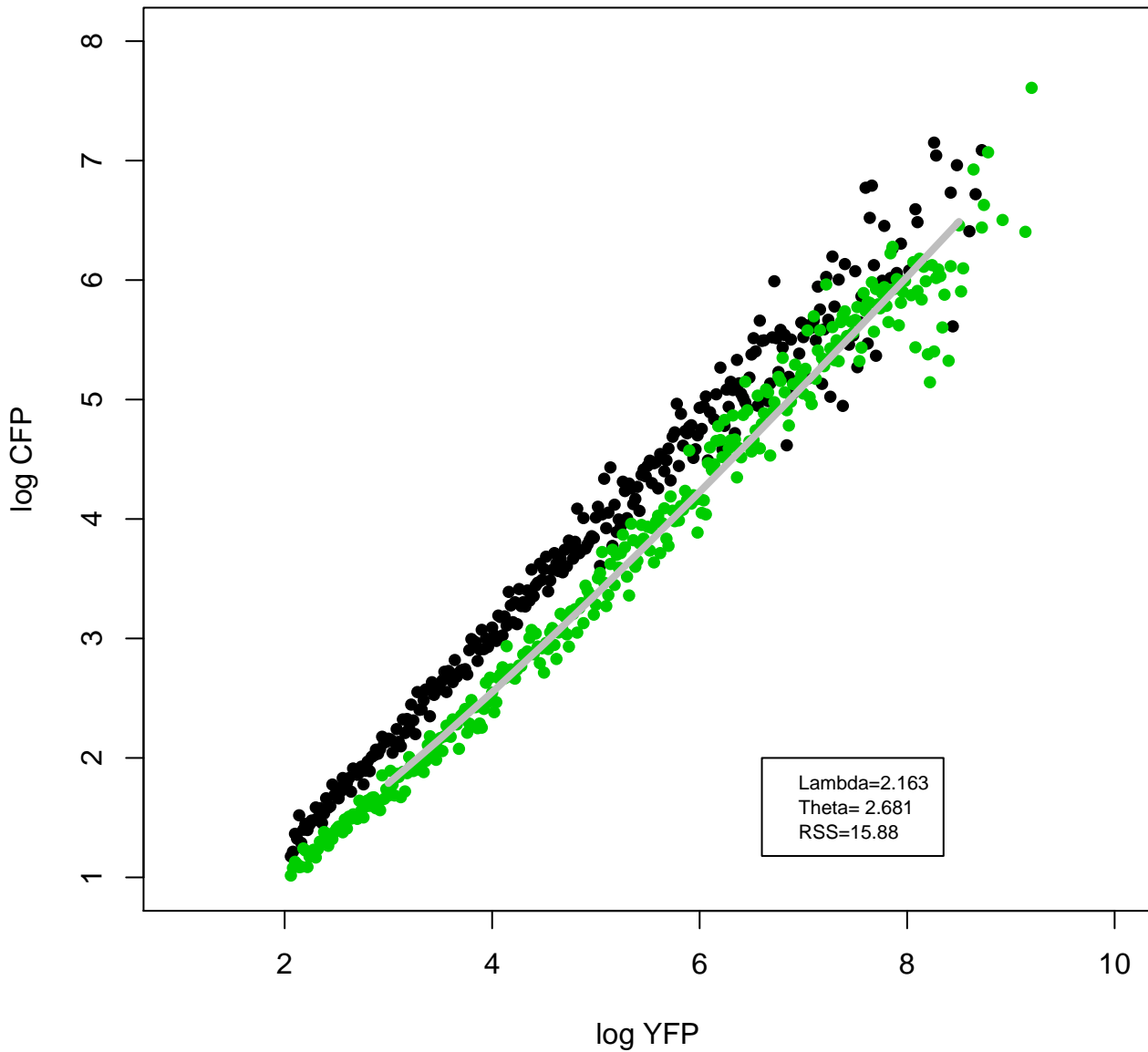
hsa-miR-24-3p



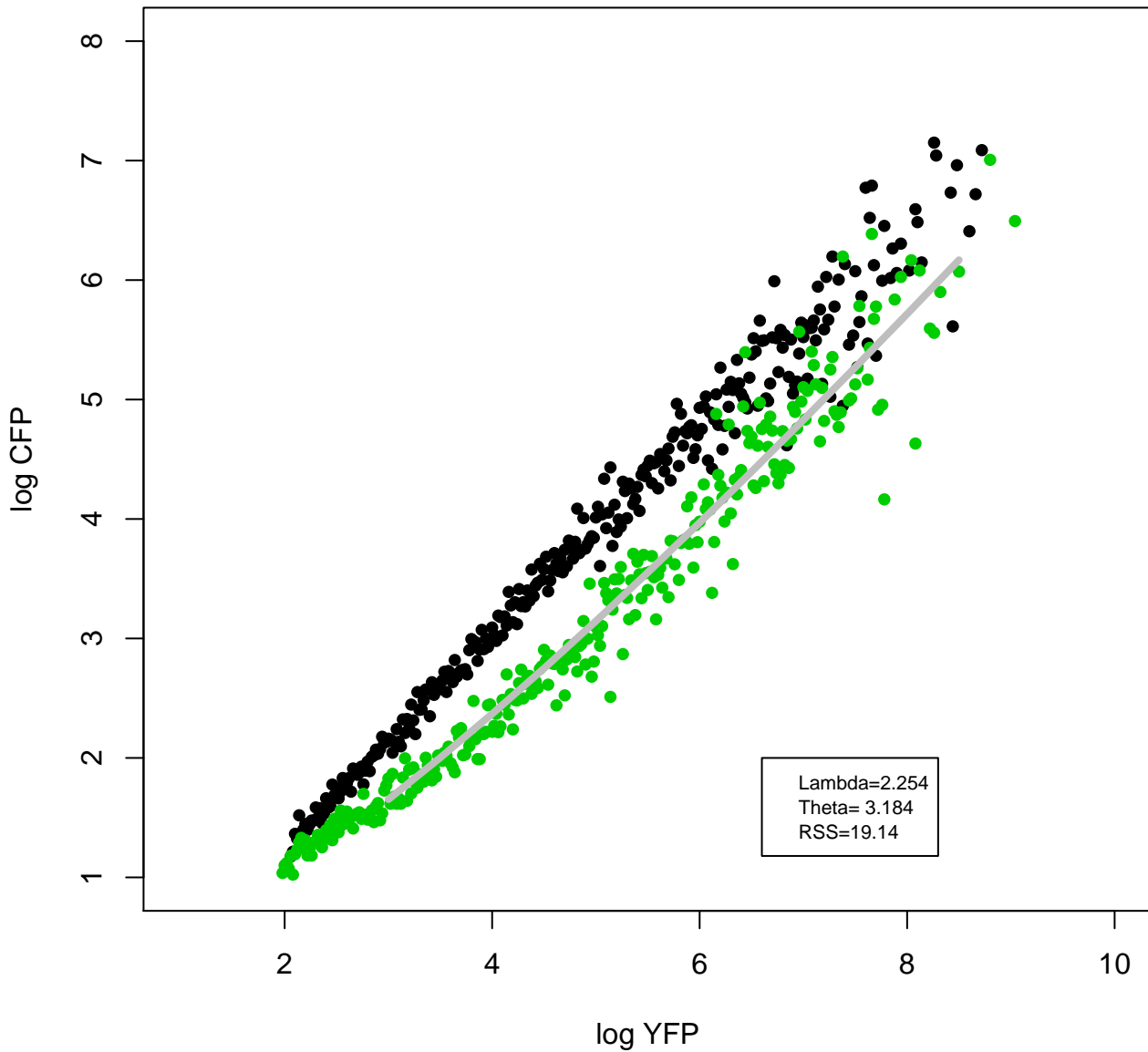
miR-26a-5p



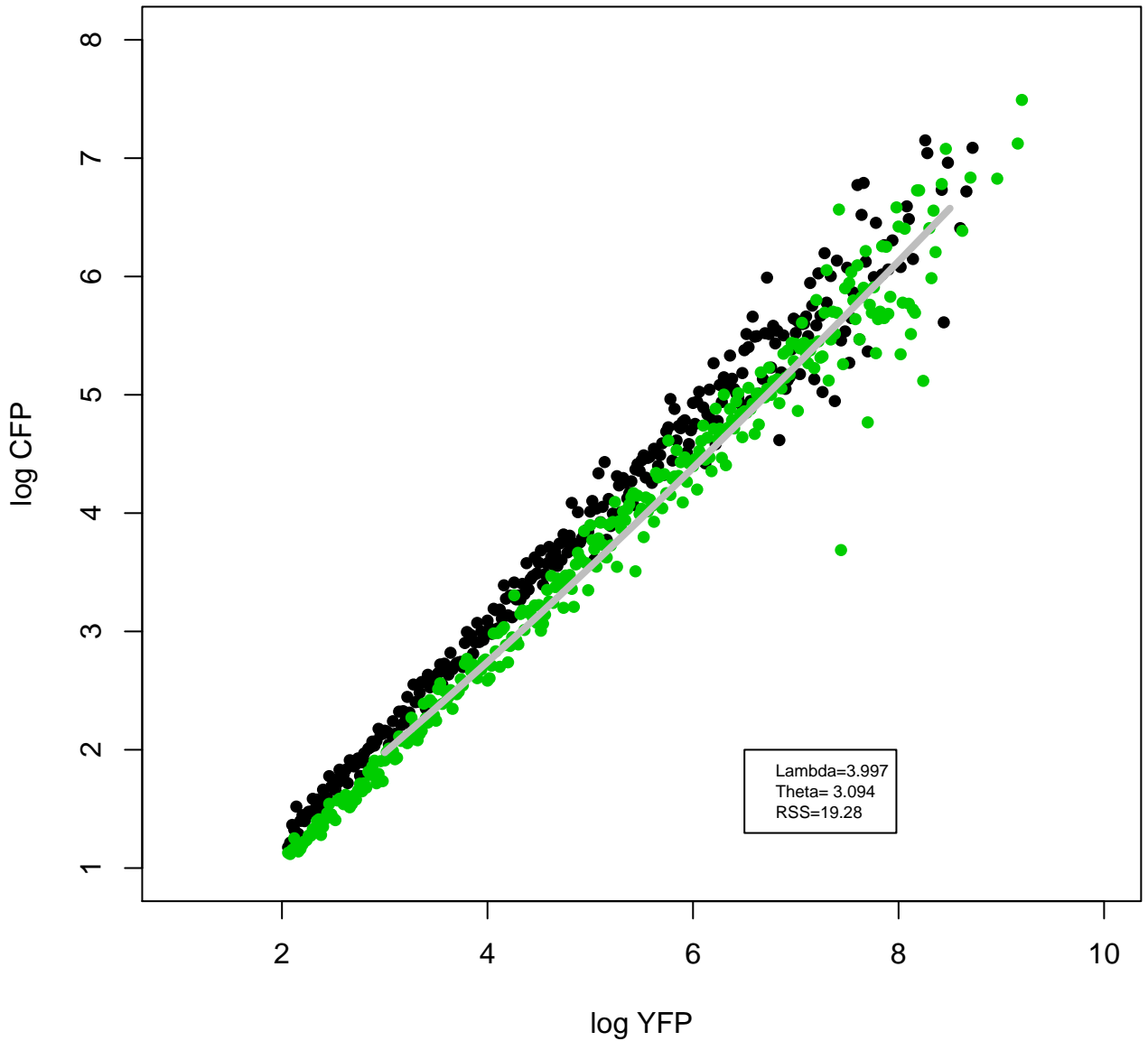
hsa-miR-29a-3p



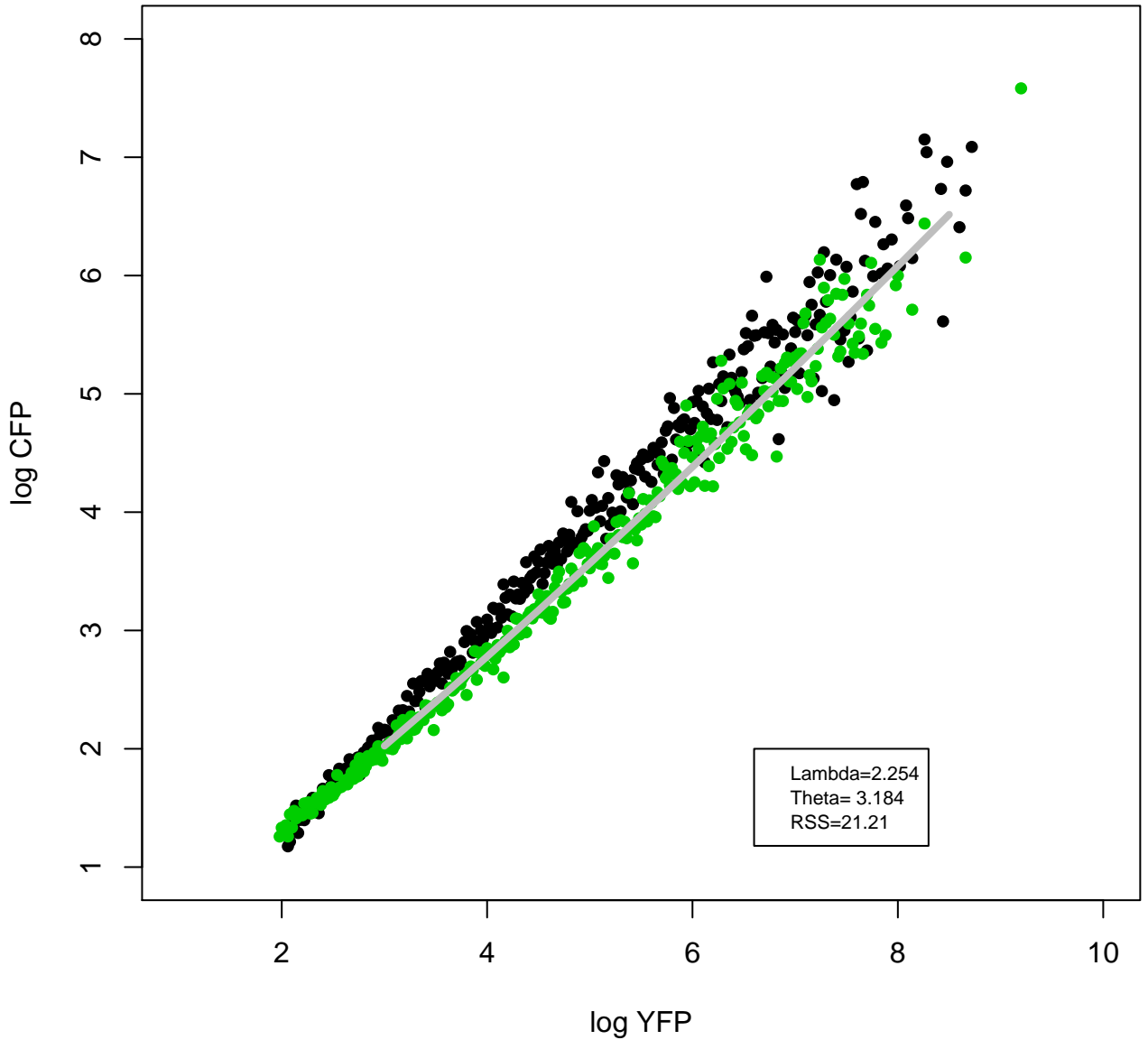
miR-340-5p



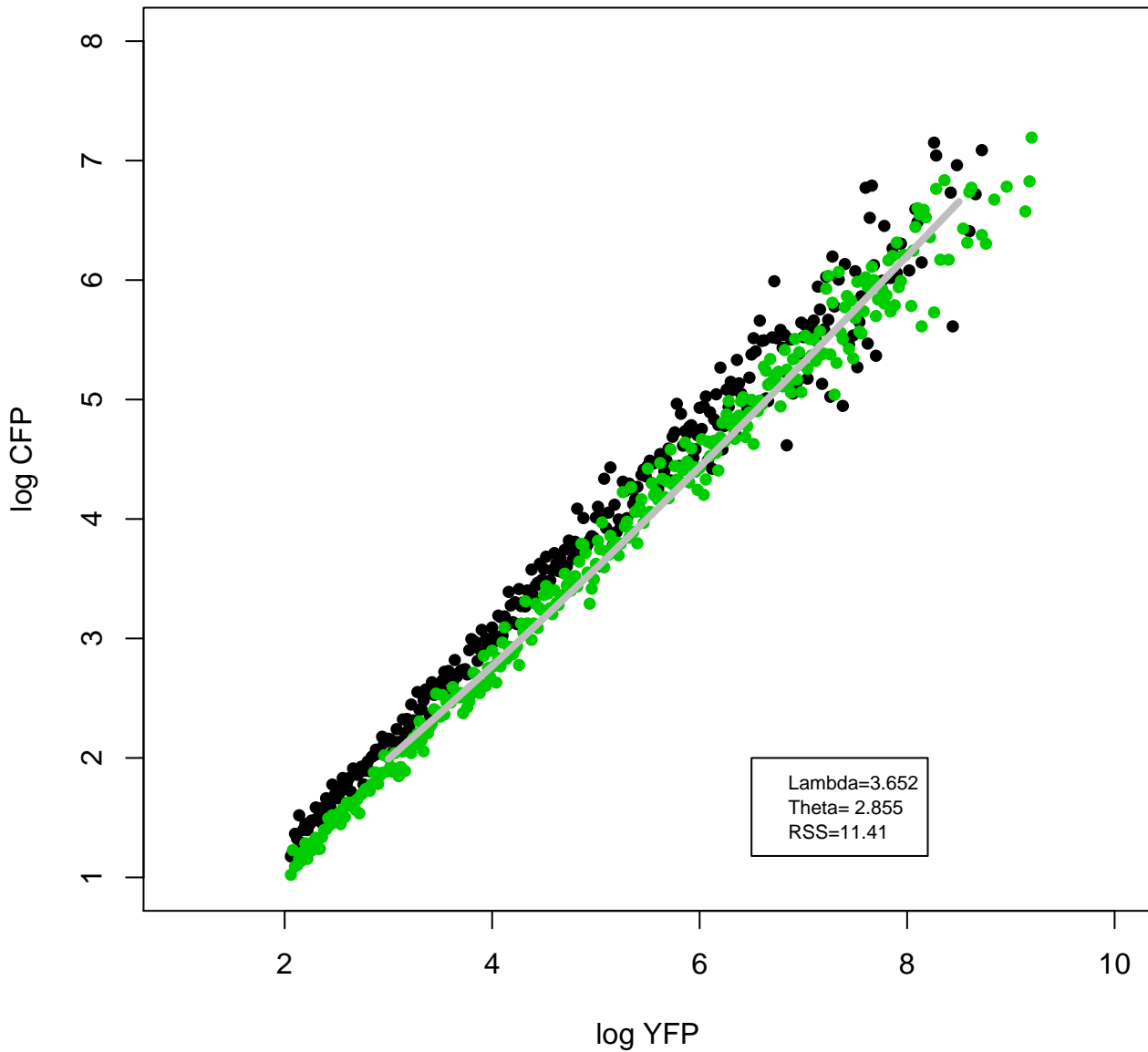
hsa-miR-100-5p



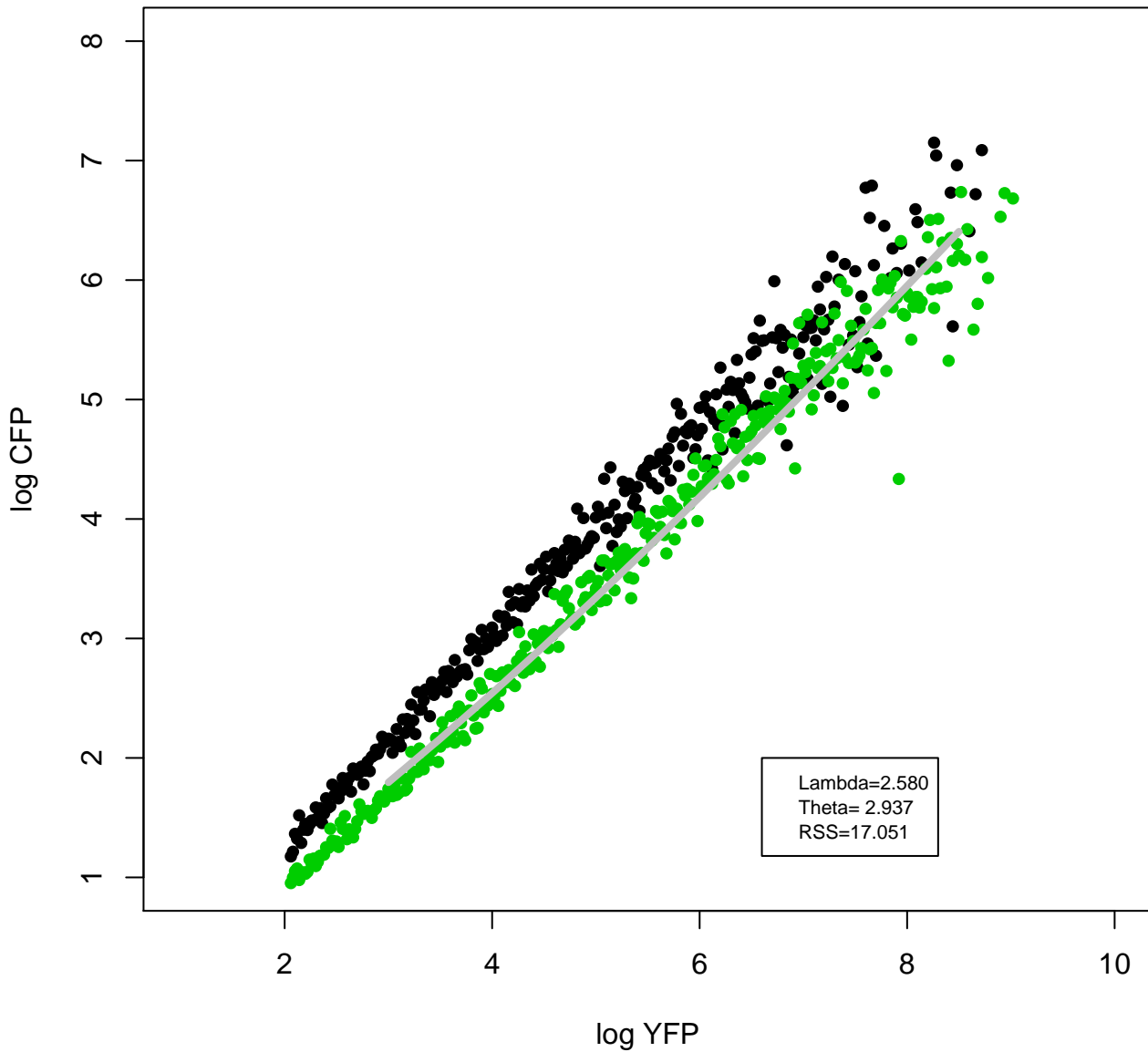
hsa-miR-125a-5p



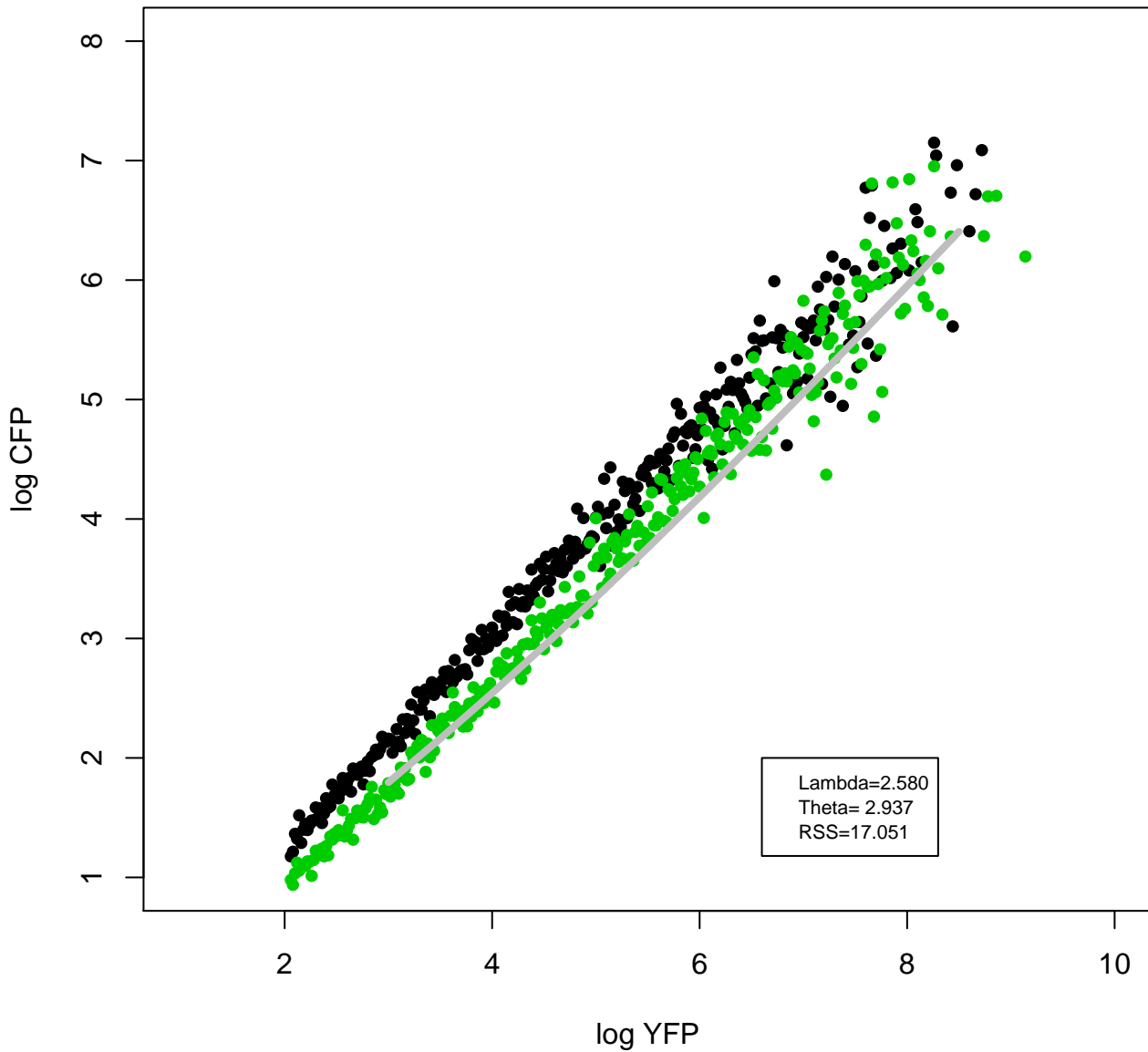
hsa-miR-1301-3p



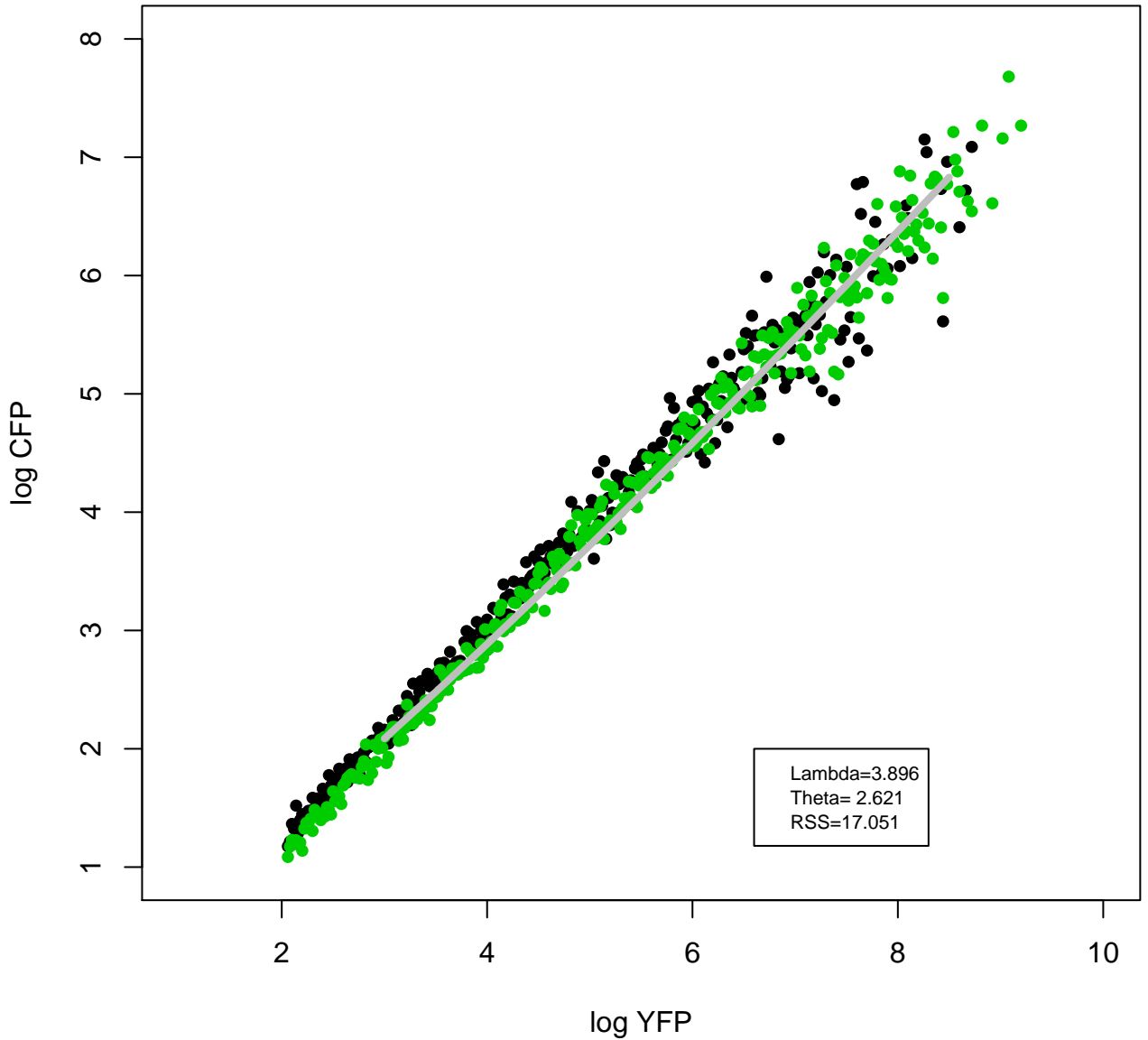
hsa-miR-215-5p



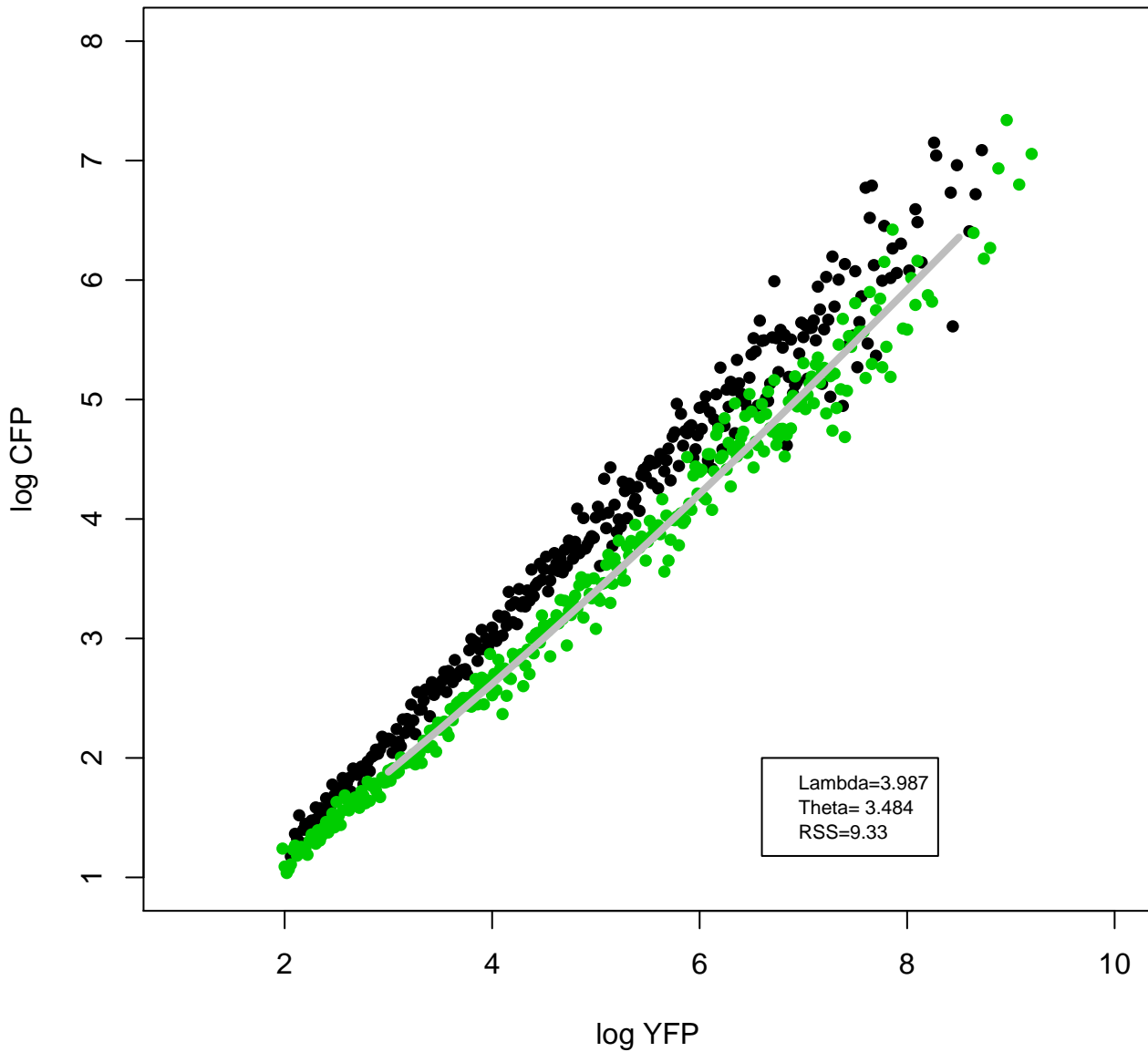
hsa-miR-23a-3p



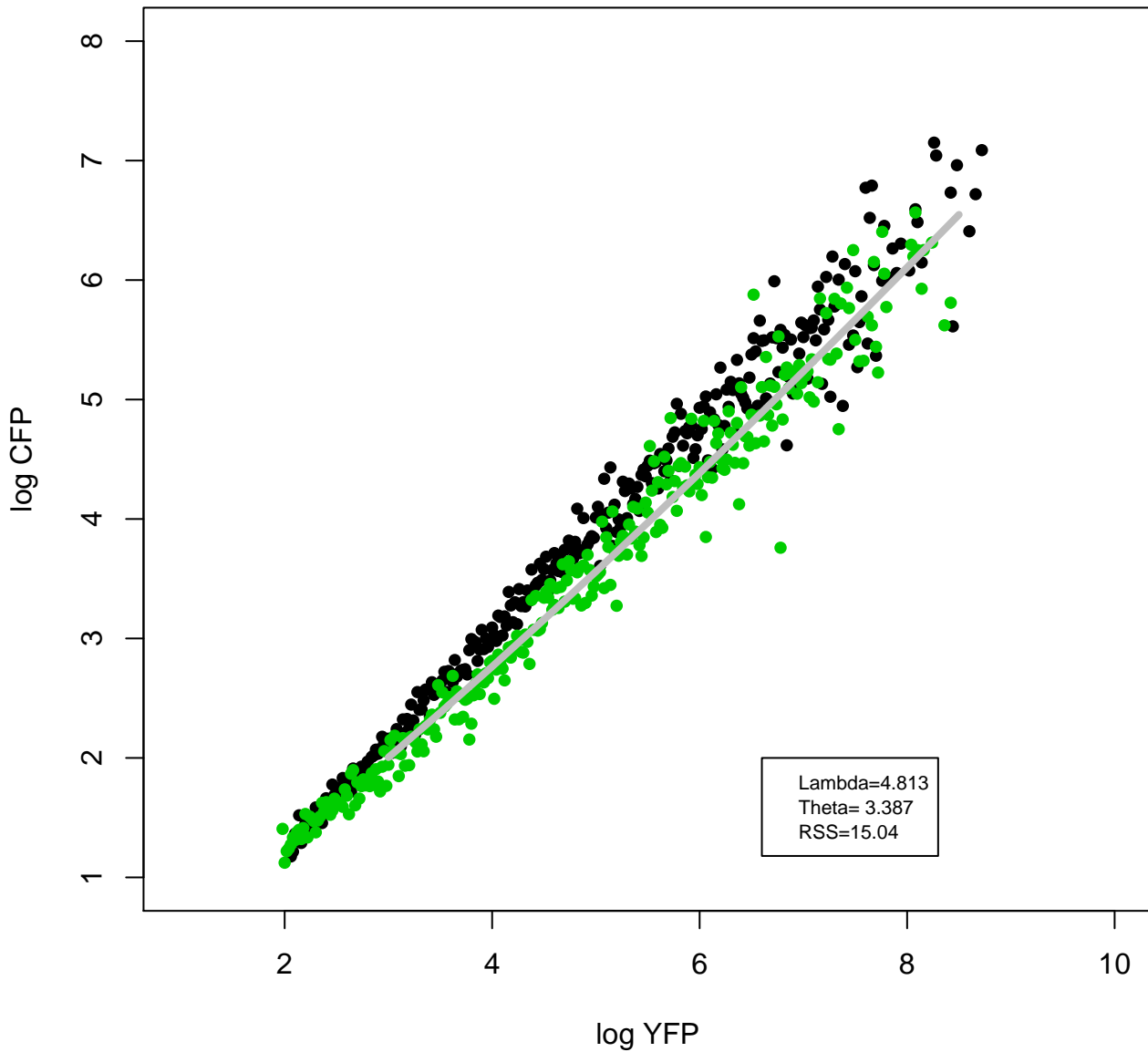
hsa-miR-28-3p



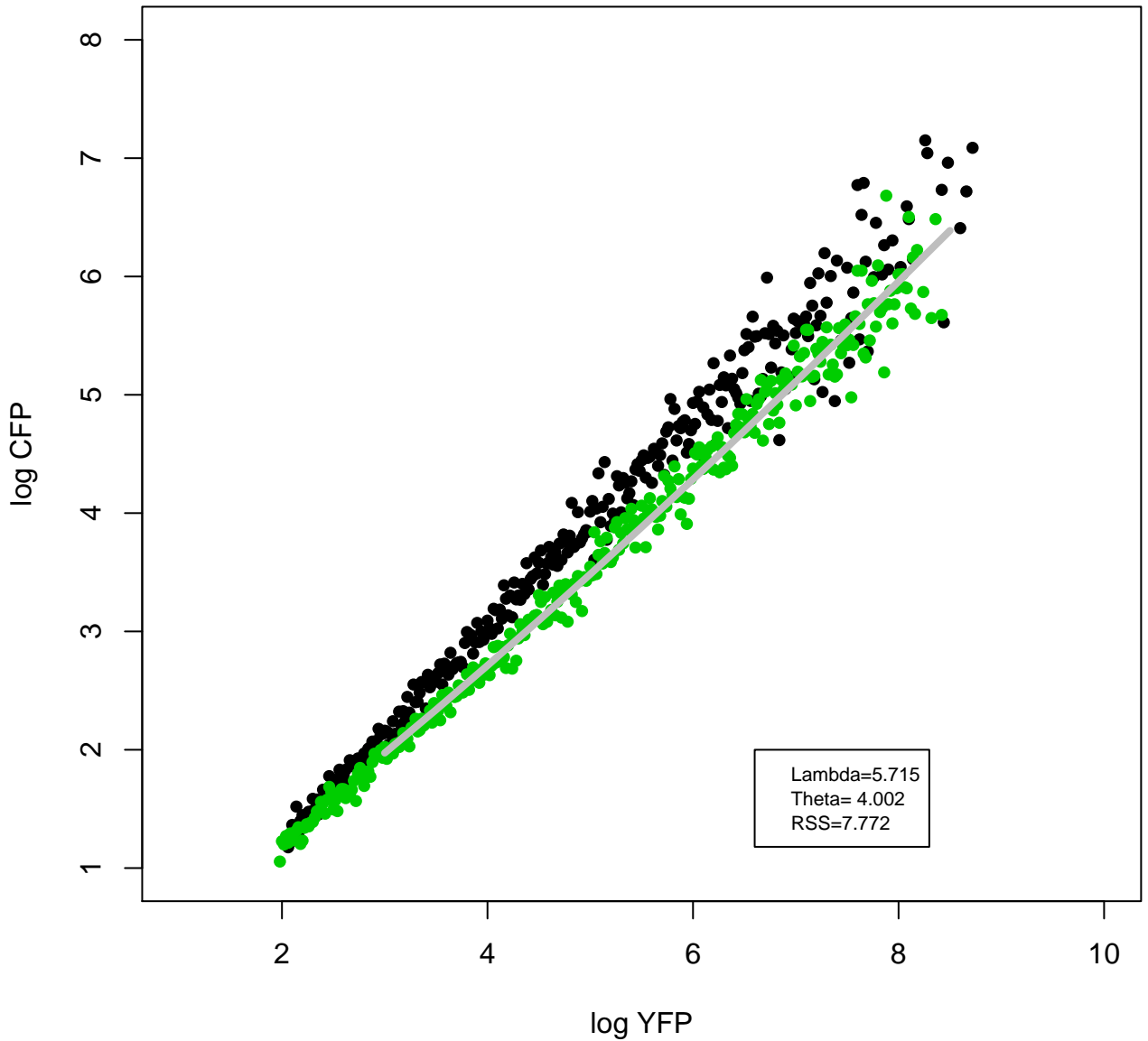
hsa-miR-3607-5p



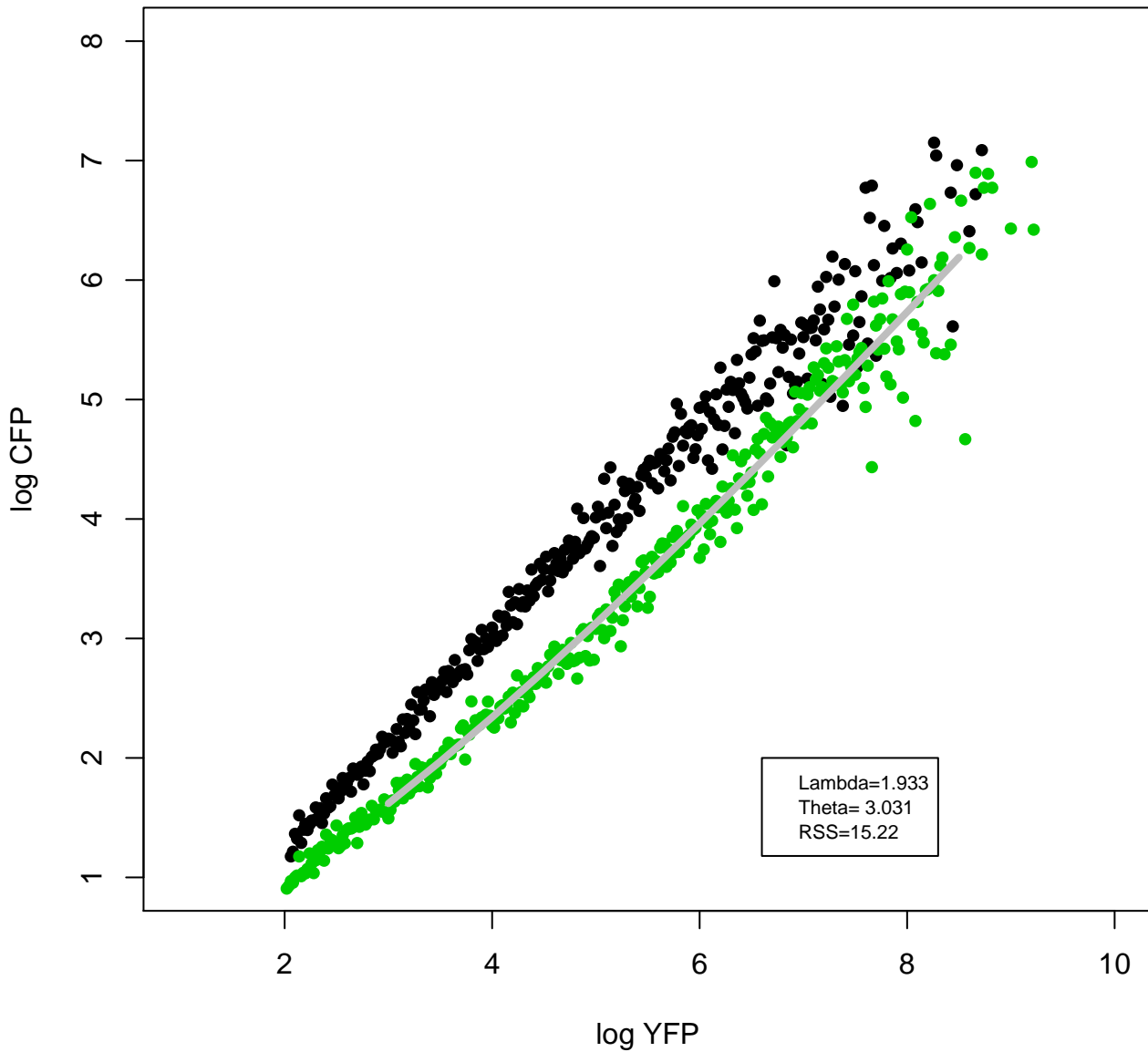
hsa-miR-500a-5p



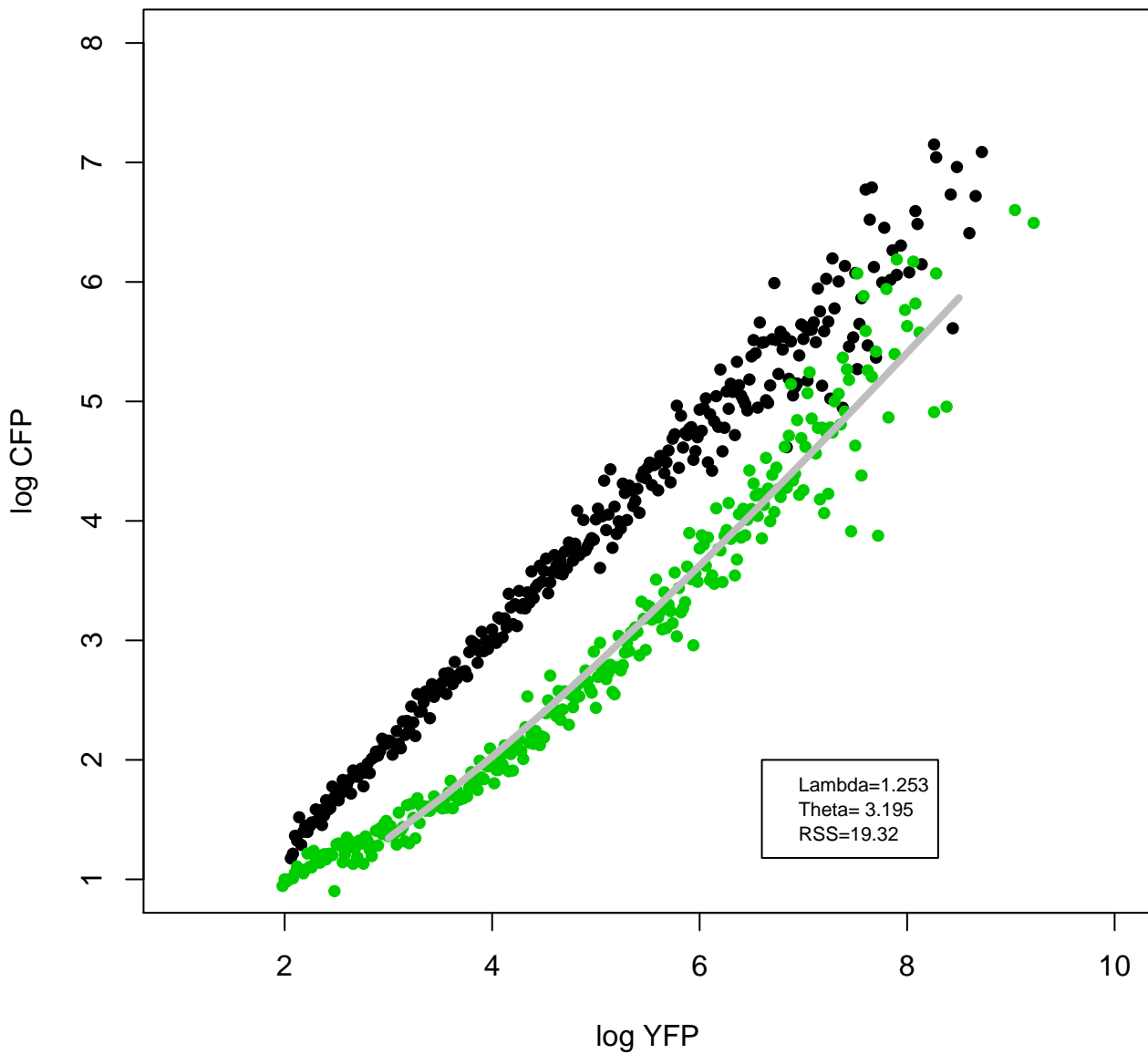
hsa-miR-671-5p



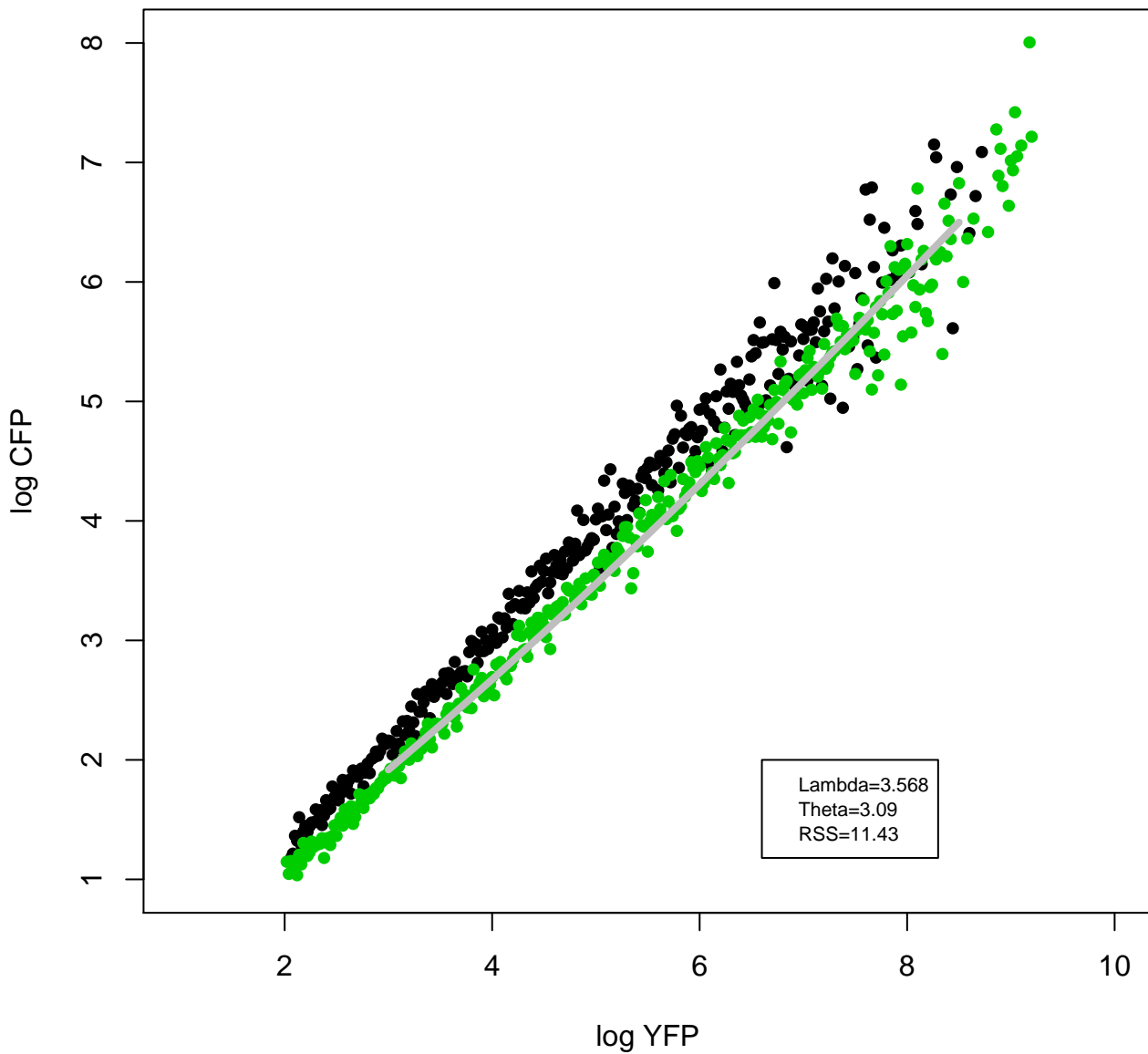
hsa-miR-29b-3p



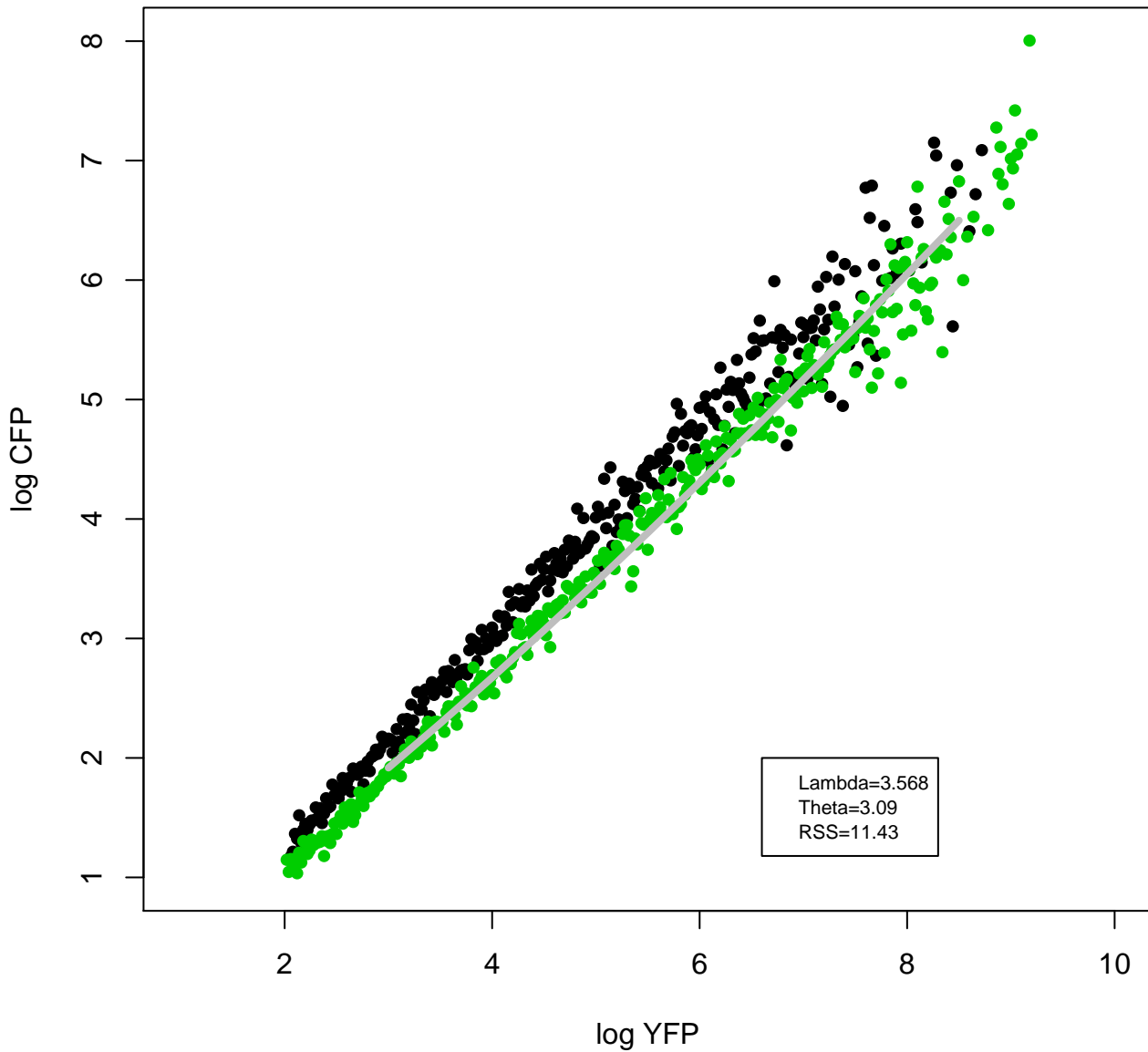
hsa-miR-103a-3p



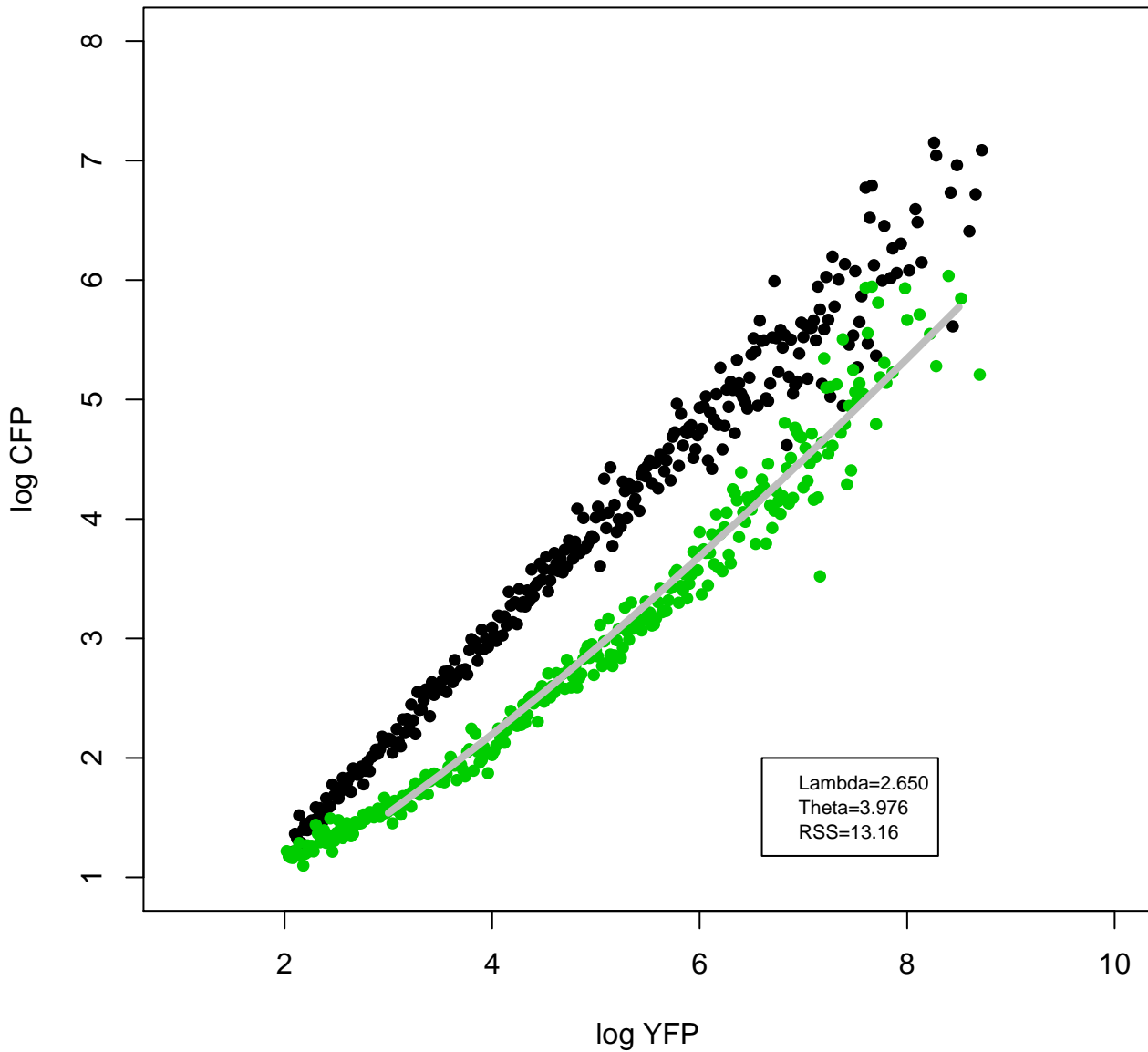
hsa-miR-3607-3p



hsa-miR-3607-3p



hsa-miR-27a-3p



hsa-miR-451a

